DEVELOPMENT OF A CHEMICAL IONIZATION MASS SPECTROMETRY TECHNIQUE FOR THE DIRECT MEASUREMENT OF HO_2

A Thesis
Presented to
The Academic Faculty

by

Javier Sanchez

In Partial Fulfillment
of the Requirements for the Degree
Master of Science in the
School of Chemical and Biomolecular Engineering

Georgia Institute of Technology
August 2016

DEVELOPMENT OF A CHEMICAL IONIZATION MASS SPECTROMETRY TECHNIQUE FOR THE DIRECT MEASUREMENT OF HO_2

Approved by:

Dr. Nga L. Ng, Advisor
School of Chemical and Biomolecular Engineering
Georgia Institute of Technology

Dr. Athanasios Nenes
School of Chemical and Biomolecular Engineering
Georgia Institute of Technology

Dr. L. Gregory Huey
School of Earth and Atmospheric Sciences
Georgia Institute of Technology

Date Approved: July 25, 2016

ACKNOWLEDGEMENTS

I would like to thank my committee members: Dr. Athanasios Nenes, Dr. Greg Huey, and my advisor, Dr. Sally Ng, for their support and advice. There is no better group of people nor place to do this kind of work. I would also like to thank Dr. Rodney Weber for his support and challenging questions. I would especially like to thank Chris Boyd for teaching me how to do just about everything in lab, and Wing Tuet for her keen aesthetic eye and unbridled optimism. A special thank you to Dave Tanner, who is a great mentor and an excellent example of how to be a scientist and a person. I would like to thank Mike Nicovich for teaching me the fastest way to figure out if a lamp makes ozone, as well as for help with flow tube experiments. I'd like to thank Xiaoxi Liu, Dexian Chen, and Theo Nah for being great colleagues. Lastly, I'd like to thank my family and friends for their unconditional love and support.

TABLE OF CONTENTS

LIST OF TABLES

LIST OF FIGURES

SUMMARY

Hydroperoxy radicals (HO_2) play important roles in tropospheric photochemistry. Despite significant efforts in constraining HO_2 abundance, notable and variable discrepancies exist between atmospheric models and observations. Disagreements may be explained by uncharacterized chemical pathways or deficiencies in current measurement techniques, likely attributable to the indirect nature of such techniques. A direct method for measuring HO_2 would aid in accurately constraining HO_2 chemistry in the atmosphere. In this work, the feasibility of several reagent ions for the direct detection of HO_2 using chemical ionization mass spectrometry (CIMS) was explored. A direct HO_2 detection scheme using bromide as a reagent ion is proposed. Laboratory characterizations suggest that the method is selective and applicable to laboratory and ambient measurements. Ambient observations were made with a high resolution time-of-flight chemical ionization mass spectrometer in Atlanta over the month of June 2015 to demonstrate the capabilities of this direct measurement technique. Observations displayed expected diurnal profiles, reaching daytime median values of ~5 ppt between 2 p.m. and 3 p.m. local time, and displayed no obvious artifacts. Measurement sensitivities of approximately 5.1±1.0 cps/ppt for a bromide ion ($^{79}Br^-$) count rate of 10^6 cps were observed. The relatively low instrument background allowed for a 3σ lower detection limit of 0.7 ppt for 1 minute time resolution. Mass spectra of ambient measurements further support the selectivity of the Br^- ionization technique. High resolution mass spectra showed that the $^{79}Br^-(HO_2)$ peak was the major component of the signal at nominal mass-to-charge 112, suggesting high selectivity for HO_2 at this mass-to-charge. Important measurement considerations and future improvements are discussed.

CHAPTER 1

INTRODUCTION

1.1 Significance of HO_2 radicals in the atmosphere

Atmospheric chemistry is driven by reactions involving free radical species. The predominant free radical in the atmosphere is the hydroperoxy radical (HO_2), which performs several key functions in tropospheric photo-chemistry. HO_2 radicals are formed primarily from the hydroxyl (OH) radical-initiated oxidation of carbon monoxide (CO) and other volatile organic compounds (VOCs), with lesser contributions from the nitrate (NO_3) radical oxidation of VOCs, ozonolysis of alkenes, and photolysis of aldehydes (e.g. HCHO)(Geyer et al., 2003;Cooke et al., 2010;Volkamer et al., 2010;Alam et al., 2013;Stone et al., 2014). HO_2 radicals are removed by the production of peroxides (hydrogen peroxide and organic hydroperoxides), conversion to OH, or uptake onto atmospheric particle surfaces (Taketani et al., 2013;Matthews et al., 2014). HO_2 radicals act as an OH reservoir, perturb the ozone photo-stationary state, and produce peroxides, which may lead to the production of organic particle mass (Docherty et al., 2005).

1.1.1 The HO_x cycle and the oxidative power of the atmosphere

HO_2 and OH radicals are closely interrelated and often treated as their sum, known as HO_x. The HO_x cycle, which encompasses the reactions involved in converting OH to HO_2 and vice versa, is shown in Figure 1.

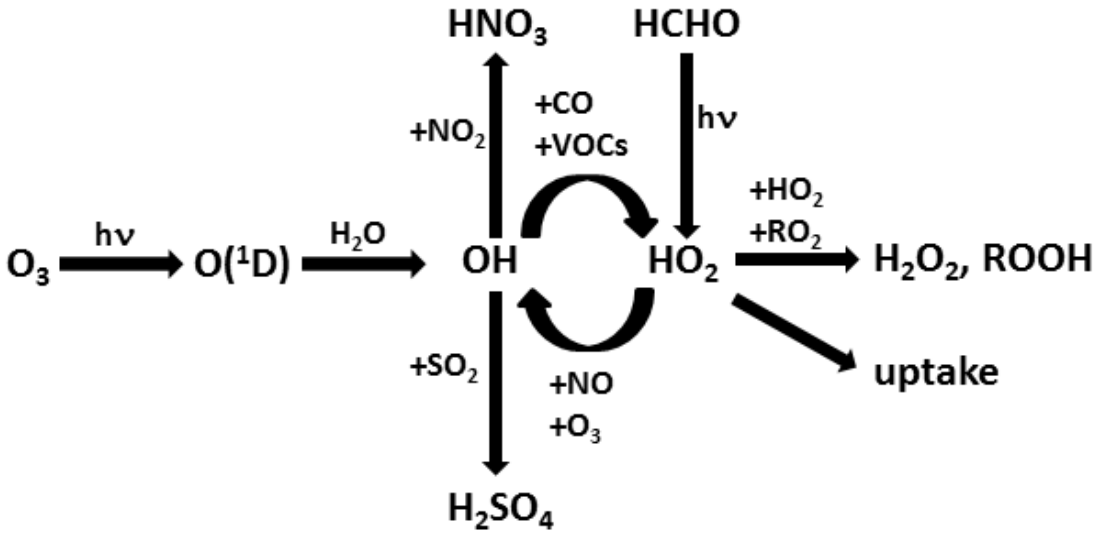

Figure 1: Simplified representation of the HOx cycle, main sources and sinks.

The rapid interconversion between HO_2 and OH allows HO_2 radicals to act as a reservoir species for OH, which is the primary daytime oxidant, and is responsible for the removal of atmospheric trace gases (e.g. CH_4). The abundance of OH determines the oxidative power of the atmosphere, which dictates the lifetime of trace gas species and their associated global warming potentials. As such, because HO_2 acts as an OH reservoir, the production and fate of HO_2 radicals strongly influences the oxidative power of the atmosphere.

1.1.2 The photo-stationary state and the HO_2 mediated production of ozone

In addition to acting as an OH reservoir, HO_2 radicals mediate ozone production in the troposphere. In the absence of competing reactions, the ozone concentration in the atmosphere is determined by the photo-stationary state (reactions 1-3),

$$NO_2 + h\nu \rightarrow NO + O(^3P) \qquad \text{(R1)}$$

$$O(^3P) + O_2 + M \rightarrow O_3 + M \quad \text{(R2)}$$

$$NO + O_3 + M \rightarrow NO_2 + M \quad \text{(R3).}$$

In the presence of HO_2 radicals, however, NO is titrated to NO_2 by reaction 4,

$$HO_2 + NO \rightarrow NO_2 + OH \quad \text{(R4).}$$

Reaction 4 competes with Reaction 3 to increase the $[NO_2]$ to [NO] ratio, increasing ozone concentration in the troposphere in regions affected by anthropogenic emissions (NO_x). A large fraction of HO_2 reacts through reaction 4.

1.1.3 HO_2 and the formation of secondary organic aerosol

HO_2 reaction with organic peroxy radicals (RO_2) produced from VOC oxidation is the primary source of atmospheric hydroperoxides. Atmospheric hydroperoxides have been shown to be important constituents of secondary organic aerosol (Docherty et al., 2005), which make up an important fraction of submicron particulate mass in the atmosphere (Kroll and Seinfeld, 2008). Particulate matter (PM) in the atmosphere has important effects on climate, health and visibility. Production of SOA is typically higher when RO_2 reacts with HO_2 radicals and lower when it reacts with NO. Therefore, the fraction of RO_2 that react with HO_2 is a key parameter in predicting climate, and remains an open question.

1.2 HO_2 measurement techniques

The importance of HO_2 radicals in the atmosphere has prompted a sizeable effort in obtaining accurate observations of HO_2 radicals in the laboratory and in the atmosphere, which remains a challenge today. A number of direct and indirect spectroscopic and spectrometric methods have been developed and employed with varying degrees of success. . The most prominent of these methods are discussed here.

1.2.1 Matrix Isolation Electron Spin Resonance

HO_2 radicals possess weak spectral lines and are present in low abundance in the troposphere. As such, HO_2 radicals have posed challenges for spectroscopic techniques. One technique which has been at least partially successful is Matrix Isolation Electron Spin Resonance (MIESR). Originally employed by Mihelcic et al. (1978) for the measurement of several free radicals, MIESR directly measures HO_2 by utilizing a deuterated water matrix at liquid nitrogen temperature (77 K) to collect HO_2 radicals for analysis using electron spin resonance. The collection of HO_2 radicals is utilized to address poor instrument sensitivity. However, the extended collection of HO_2 radicals (usually 30 minutes) results in poor time resolution, which is critical in atmospheric measurements. Nevertheless, the technique is useful as a standard for comparison of other methods.

1.2.2 Peroxy Radical Chemical Amplification

The peroxy radical chemical amplification (PERCA) technique (Cantrell and Stedman, 1982;Cantrell et al., 1984;Liu et al., 2009;Horstjann et al., 2014) was developed as a simple but indirect method of measuring HO_2. The technique can provide both sensitive and fast time response measurements of HO_2. The measurement scheme exploits radical propagation reactions (5-7) to produce NO_2 from HO_2 radicals present in the sample gas.

$$HO_2 + NO \rightarrow OH + NO_2 \qquad \text{(R5)}$$

$$CO + OH \rightarrow CO_2 + H \qquad \text{(R6)}$$

$$H + O_2 + M \rightarrow HO_2 + M \qquad \text{(R7)}$$

NO and CO are added in large concentrations and sample HO_2 is continuously recycled to produce NO_2. NO_2 has then been traditionally detected using liquid-phase luminescence from the reaction of luminol with NO_2, though recent methods utilize cavity ring-down spectroscopy. Because multiple NO_2 molecules are formed from each HO_2 radical in the sample, the signal is effectively amplified. A significant drawback to the technique is that sufficient reaction time is required to effectively amplify the signal, as will be discussed later.

1.2.3 ROx Chemical Conversion and Peroxy Radicals Chemical Ionization Mass Spectrometry

ROx Chemical Conversion chemical ionization mass spectrometry (ROxMAS) and peroxy radical chemical ionization mass spectrometry (PerCIMS) (Hanke et al., 2002;Edwards et al., 2003;Hornbrook et al., 2011;Kim et al., 2013;Wolfe et al., 2014) measure HO_2 radicals through the indirect chemical titration of HO_2 radicals to sulfuric acid and subsequent ionization to HSO_4^- for transmission and detection by a mass spectrometer. The reaction scheme for the chemical titration of HO_2 is as follows:

$$HO_2 + NO \rightarrow OH + NO_2 \quad \text{(R8)}$$

$$OH + SO_2 + M \rightarrow HSO_3 + M \quad \text{(R9)}$$

$$HSO_3 + O_2 \rightarrow SO_3 + HO_2 \quad \text{(R10)}$$

$$SO_3 + 2H_2O \rightarrow H_2SO_4 + H_2O \quad \text{(R11)}$$

$$H_2SO_4 + NO_3^- \rightarrow HSO_4^- + NO_3 \quad \text{(R12).}$$

The technique requires precise control of reaction time but provides low detection limits at fast time resolution. The NO_3^- reagent is selective and effectively ionizes sulfuric

acid. Isotopic $^{34}SO_2$ is often used for chemical titration to produce $H^{34}SO_4^-$ in order to distinguish sulfuric acid produced by the titration of HO_2 from atmospheric sulfuric acid.

1.2.4 Fluorescence Assay Gas Expansion Laser Induced Fluorescence

The Fluorescence Assay Gas Expansion Laser Induced Fluorescence (FAGE-LIF) (Stevens et al., 1994;Brune et al., 1995;Griffith et al., 2013;Walker et al., 2015) technique is the most commonly used method to measure HO_2 in the atmosphere, in large part due to its relative simplicity, low detection limits, and fast time resolution. In FAGE-LIF, HO_2 radicals are titrated to OH by the addition of NO (reaction 8) in the sample line. The resulting OH is then measured by laser excitation at 308 nm.

1.2.5 Indirect methods and artifacts

Unlike MIESR, which is a direct measurement method, PERCA, PerCIMS, and LIF rely on the chemical titration of HO_2 radicals by adding large amounts of NO to the sample gas stream. The addition of NO introduces serious complications in these measurement schemes. Organic peroxy radicals (RO_2), which are present in the atmosphere, react analogously with NO to produce an alkoxy radical and NO_2 (reaction 13).

$$RO_2 + NO \rightarrow RO + NO_2 \qquad \text{(R13)}$$

The RO radical then reacts with O_2 via Reaction 14,

$$RO + O_2 \rightarrow R'O + HO_2 \qquad \text{(R14).}$$

The reaction of alkoxy radicals produces HO_2, which results in a significant artifact in the HO_2 measurement. Further reactions of R'O may also result in the production of additional HO_2. Due to its relatively long reaction time, the PERCA technique is efficient in converting RO_2 to HO_2 such that it is a useful technique for the

measurement of total [RO_2+HO_2]. However, this technique cannot speciate HO_2 from total peroxy radical measurements, though previous attempts have been made (Miyazaki et al., 2010).

PerCIMS measurements suffer from similar artifacts. Because reaction 14 requires oxygen, Hornbrook et al. (2011) attempted to modulate the relative NO to O_2 ratio in the reaction region to suppress HO_2 generation from RO_2. The oxygen dilution modulation scheme was successful in suppressing HO_2 generation from small saturated hydrocarbons. However, in the case of larger alkanes or unsaturated hydrocarbons, such as isoprene or aromatic compounds, the scheme does not effectively suppress HO_2 generation, as the unimolecular decomposition or isomerization pathways available to these species do not require oxygen for the production of HO_2.

Unlike PERCA and PerCIMS, which require long reaction times and multiple conversion steps, respectively, the FAGE-LIF technique requires minimal reaction time between HO_2 and NO. Accordingly, the reaction time can be optimized to fully convert HO_2 and minimize RO_2 conversion. Nevertheless, the same artifacts have been observed in LIF instruments (Fuchs et al., 2011;Whalley et al., 2013).

The HO_2 yield from RO_2+NO reactions depends on the hydrocarbon precursor, which makes it unlikely that one can reliably post-correct measurements for contributions of RO_2 radicals, as this would require speciated measurements of all VOCs present in sufficient concentrations in the sample gas. Even if all VOC measurements were available, measurement uncertainties would introduce large errors in the HO_2 concentration.

1.3 Discrepancies in model-measurement comparisons of HO_2

Current understanding of tropospheric photo-chemistry in different environments is evaluated by model-measurement comparison of key atmospheric species. Numerous field studies have been conducted to measure HO_2 and constrain its sources and sinks. Large discrepancies have been observed between modeled HO_2 and observed HO_2 mixing ratios in several environments. The measured to model ratios of HO_2 (and OH) have been found to be highly variable (Stone et al., 2012). Observed discrepancies in HO_2 abundance has led to density functional theory and laboratory studies in an attempt to identify new chemical pathways which may explain differences between modeled and measured HO_2 and OH (J. Peeters, 2009;Crounse et al., 2011). New chemical pathways have been discovered, but these have not closed the model-measurement gap.

It is entirely possible, and likely, that the observed gaps are not only due to undiscovered chemical pathways, but to measurement artifacts as well. The indirect nature of current HO_2 radical measurements and further complications resulting from reactions of NO with organic peroxy radicals could play a major role in the observed discrepancy.

1.4 Purpose of this work

Given the uncertainties associated with indirect methods of HO_2 measurement and the time resolution required for atmospheric measurements, a direct fast time resolution measurement of HO_2 would benefit efforts aiming to measure and model HO_2 in order to understand atmospheric photochemistry. In this work, a number of reagent ions are evaluated with respect to their potential use for the direct detection of HO_2 using a chemical ionization mass spectrometer. A clustering ionization scheme is proposed using

Br^- reagent anions to produce $Br^-(HO_2)$ adducts. The technique's sensitivity and selectivity are presented, as well as the effect of humidity and temperature. Ambient measurements were conducted over the month of June, 2015 in Atlanta to demonstrate the capability of the technique in providing ambient measurements of HO_2. Important considerations regarding instrument backgrounding methods and future method optimization are also discussed.

CHAPTER 2

METHODS

2.1 Instrument description

The work described was performed using both a High Resolution Time-of-Flight Chemical Ionization Mass Spectrometer (HR-ToF-CIMS, Aerodyne Research, Inc.) and a house-built quadrupole CIMS. The HR-ToF-CIMS consists of an atmospheric pressure interface with five differentially pumped stages. The initial stages are pumped utilizing SH-112 and TriScroll 600 dry scroll pumps. The pressure is decreased further in the following stages by using a multi-stage turbomolecular pump, which is backed by a Vacuubrand MD1 diaphragm pump. The instrument design has been described in detail by Bertram et al. (2011). Figure 2 shows a schematic diagram of the HR-ToF-CIMS.

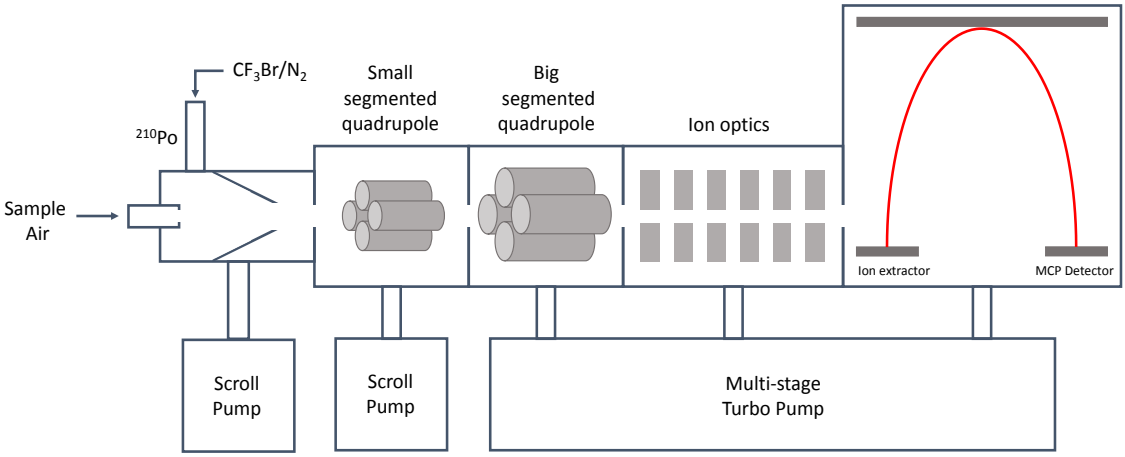

Figure 2: Schematic diagram of the High Resolution Time-of-Flight Chemical Ionization Mass Spectrometer. Sample air enters the flow tube through a 0.5 mm orifice where it is ionized at 100 mbar. The contents of the ion-molecule reaction region are sub-sampled through a 0.3 mm orifice into the small segmented quadrupole (SSQ) chamber held at 2.5 mbar. Collisional dissociation occurs in the SSQ. Ion products are then collimated by the big segmented quadrupole (BSQ) where they also dissipate energy by collisions with

background gas at reduced pressure. The subsequent ion lenses then focus and accelerate the ion beam towards the ToF analyzer.

HO_2 is measured by introducing 2 sLPM of sample gas through at 0.5 mm critical orifice into the ion-molecule reaction region. Br^- reagent ions are produced by flowing 5-10 sccm of a 0.2% CF_3Br/N_2 mixture carried by 2 sLPM N_2 gas (99.999%, Airgas) through a 10 mCi ^{210}Po alpha radiation source. Electrons are generated by alpha-particle collisions with N_2 molecules and captured by CF_3Br to form Br^- and CF_3 radicals. The ion-molecule reaction region has a residence time of 0.07 seconds and is operated at a pressure of 100 mbar. HO_2 radicals present in the sample gas collide with Br^- to form $Br^-(HO_2)$ adducts. The contents of the IMR were sub-sampled through a 0.3 mm critical orifice leading to a small sectioned quadrupole which acts as a collision cell, where soft collisions prevent excessive clustering of ions and molecules. The product ions are then collimated by a larger quadrupole. Ion products also dissipate energy in the large quadrupole by collisions with background gas. Ion lenses then focus and accelerate the ion beam towards the time-of-flight analyzer, where products are speciated based on the time required for the product ion to reach a multi-channel plate detector. The isotopic abundance of bromine is such that the adduct is detected at two nominal mass-to-charge ratios, *m/z* 112 and *m/z* 114 corresponding to the ^{79}Br and ^{81}Br isotopes, respectively. These adducts have fractional mass-to-charge ratios of 111.9165 and 113.9144 Th. In order to demonstrate the generalizability of the technique to instruments with unit mass resolution, only the unit mass resolution data are used in this paper, though the high resolution capabilities were utilized to diagnose and address potential artifacts during method development. High resolution mass spectra were also used to unambiguously

identify $Br^-(HO_2)$. In contrast to the HR-ToF-CIMS, the quadrupole CIMS was operated at an ion-molecule reaction region pressure of 15 torr. The sample and N_2 flow rates were both 2 sLPM in that instrument.

2.2 HO_2 radical generation

HO_2 radicals were generated for evaluating chemical ionization reagent ions and for instrument calibrations by the photolysis of water at 184.9 nm. A mercury UV lamp which emitted primarily at 185 and 254 nm was used as the UV light source. The water photolysis technique has been used and is described by a number of previous studies, e.g. (Tanner et al., 1997;Holland et al., 2003;Smith et al., 2006;Dusanter et al.). Pure air from a pure air generator (AADCO 747-14) was humidified by passing the gas stream through glass bubblers. The high humidity gas was then diluted in dry pure air to vary the relative humidity of the gas. The gas stream was then introduced into a black anodized aluminum square flow tube (15.6 mm × 15.6 mm× 520 mm) and exposed to UV radiation through a small slit. HO_2 concentrations were calculated using Eq. (1),

$$\Delta[HO_2]=\phi\sigma I[H_2O]\Delta t, \quad (1)$$

where ϕ, σ, I, and Δt represent the quantum yield, water absorption cross-section, UV lamp photon flux at 184.9 nm, and irradiation time, respectively. The quantum yield was assumed to be unity and a value of 7.22 x 10^{-20} cm^2 was used for the water absorption cross section (Creasey et al., 2000). The lamp photon flux was measured using a Hamamatsu Phototube (Hamamatsu Photonics), and found to be 2.6 x 10^{13} photons cm^{-2} s^{-1}. A bandpass filter (HORIBA Scientific) was used to selectively transmit at 185 nm, significantly reducing the lamp emission at 254 nm to minimize ozone photolysis. The dew point of the gas was measured using a LICOR LI-840A CO_2/H_2O gas analyzer. The

irradiation time was calculated based on the flow velocity which was measured using a Dwyer pitot tube and a magnehelic pressure sensor. Flow velocities varied between 400-800 cm/s (Re > 4000) to promote plug flow conditions and ensure a uniform HO_2 radical concentration profile within the aluminum tube. The lamp was located at a distance greater than 10 times the hydraulic diameter from the entrance of the tube to allow the flow profile to fully develop. Plug flow conditions were confirmed by measuring the flow velocity both at the center line and near the walls of the tube, showing no measureable differences. The water vapor mixing ratios were varied between 0.66 and 8.20 parts per thousand. The time before introduction into the instrument, after production of HO_2, was minimized (τ~60 ms) to avoid additional HO_2 generation from OH oxidation of trace CO which may be present in the N_2 gas. It was calculated that less than 8% of the OH formed would react with CO to produce additional HO_2 assuming a CO concentration of 500 ppb. Addition of 40 ppm of C_3F_6 as OH scavenger had no effect on HO_2 signal intensity, confirming the lack of contribution from OH oxidation to HO_2. The HO_2 concentration was kept low (2-45 ppt) to calibrate for the HO_2 levels observed during ambient sampling and to avoid non-linearity in the calibration curve due to depletion of HO_2 through HO_2 radical-radical recombination. At the HO_2 mixing ratios employed, less than 1% of HO_2 are estimated to be lost to recombination. The overall calibration uncertainty is 18% (1σ). The contribution of the different parameters in Equation 1 to the overall uncertainty is given in Table 1.

Table 1: Contribution of all parameters used during the calibration for determining instrument sensitivity.

Parameter	**Uncertainty (1σ %)**
$\sigma_{water,184.9\ nm}$	3
I	17
$[H_2O]$	1.5
Δt	3
S_{HO2}	3
Total calibration uncertainty	**18**

A conservative estimate of 20% is used in this work.

2.3 Reagent ion evaluation and laboratory characterizations

Several reagent ions were evaluated with respect to their ability to sensitively and selectively measure HO_2. The reagent ions evaluated were O_2^-, SF_6^-, Cl^-, I^-, and Br^-. O_2^- and SF_6^- were chosen due to their low electron affinities, the latter having been used previously for laboratory and ambient measurements of numerous species (Huey et al., 1995;Slusher et al., 2001). Species with low electron affinities are more likely to undergo charge transfer ionization, which would result in the production of HO_2^- as a product ion in this particular case.

I^- was chosen due to previous observations which suggested its potential application to HO_2 radical measurements (Veres et al., 2015). Cl^- and Br^- were also evaluated due to their similarity to I^- but different electron affinities and molecular weights. Reagent ions, along with their respective sources are summarized in Table 2.

Table 2: Summary of reagent ions evaluated, corresponding expected product ions, and reagent ion source mixtures.

Reagent ion	Expected product ion	Source mixture
O_2^-	HO_2^-	Pure air
SF_6^-	HO_2^-	0.2 % SF_6/N_2
Cl^-	$Cl^-(HO_2)$	HCl (in vial), 10 sccm N_2 carrier gas
I^-	$I^-(HO_2)$	0.2% CH_3I/N_2
Br^-	$Br^-(HO_2)$	0.2% CF_3Br/N_2

Reagent ion laboratory characterizations involved the generation of HO_2 radicals utilizing the procedure described in Sect. 2.2. Unlike during instrument calibrations, where HO_2 radical levels were below 50 ppt, HO_2 radical levels exceeded 300 ppt during reagent ion evaluations. The instrument background for signals corresponding to HO_2 radicals were obtained by adding large concentrations of NO (2-4 ppm). Because a limited number of species react with NO, a decrease in signal from NO addition confirms the identity of the signal cluster, in that it likely corresponds to HO_2 radicals. Smaller concentrations of NO (ppb level) were also added, and the reaction time estimated, to determine whether NO kinetics of the observed signals were consistent with those expected from HO_2 radicals based on the literature rate constant for reaction 8. During reagent ion evaluations, the sample was not humidified in addition to the water added for the photolysis of water, nor was additional water vapor added to the IMR, for simplicity.

2.4 Ambient measurements

To demonstrate the applicability of the Br^- ionization scheme to ambient HO_2 measurements, a field study was conducted in June, 2015 (6/9/2015-6/25/2015) in

Atlanta at an urban background site located on the roof (30-40 m above ground) of the Ford Environmental Science & Technology building on the Georgia Tech campus, which has been used for previous ambient studies (Hennigan et al., 2008;Xu et al., 2015a;Xu et al., 2015b). The site is about 840 m west of Interstate-75/85 and can therefore be affected by traffic emissions. The instrument was located outside in an enclosure, allowing for a short 1 cm inner diameter Teflon^{TM} inlet of approximately 13 cm in length. The residence time of ambient sample in the tube was short (0.3 seconds) which helps to minimize HO_2 surface losses on the sample tubing. Data was collected at a 1 Hz frequency and averaged to 1 minute. A solenoid valve was used to perform periodic additions of 10 sccm of an NO/N_2 mixture (Scott-Marrin, 810 ppm) into the sample stream every 10 minutes on a 10% duty cycle to obtain the measurement background. The *m/z* 112 signal was normalized to a $^{79}Br^-$ count of 10^6 cps to account for temporal changes in reagent ion abundance.

Various co-located instruments were deployed for simultaneous measurements of O_3, NO, NO_2, and HNO_4. NO concentrations were measured using a Teledyne 200EU chemiluminescence monitor while NO_2 was measured by a Cavity Attenuated Phase Shift NO_2 monitor (Aerodyne Research, Inc.). Ozone was measured using a Teledyne Model T400 UV absorption analyzer. Pernitric acid (HNO_4), formed from the reaction of HO_2 with NO_2 was also monitored using a house-built Quadrupole Chemical Ionization Mass Spectrometer (Q-CIMS) with an Iodide-adduct ionization scheme and observed at *m/z* 206. A similar configuration of the instrument has been described previously by Slusher et al. (2004), and previous measurements of HNO_4 using I^- have been conducted by Veres et al. (2015). Meteorological data, including temperature and humidity, were

recorded using a Vantage Pro2 weather station. An additional UV sensor was employed with the Vantage Pro2 weather station to obtain an UV index measurement between 280 and 360 nm.

CHAPTER 3

RESULTS

3.1 Reagent ion evaluation

O_2^- and SF_6^- reagent ions were utilized in an attempt to produce the HO_2^- ion directly via charge exchange. However, HO_2^- was not detected in laboratory characterization utilizing either reagent. It is likely that the HO_2^- ion forms but is rapidly consumed in secondary reactions due to its low electron affinity (Ramond et al., 2002), which results in high reactivity. The SF_6^- ionization of HO_2 does produce a cluster at mass-to-charge 52, which was unambiguously assigned using the HR-ToF-CIMS as HO_2F^- in the high resolution mass spectrum. However, the signal was not quantitatively reproducible. Additionally, the form of the cluster is more likely to be O_2^-(HF) than $F^-(HO_2)$ (Seeley et al., 1996), which may compromise the selectivity of the measurement, as O_2^- ions are not unique to the ionization of HO_2. Furthermore, SF_6^- hydrolyses readily (Arnold and Viggiano, 2001), which may prove to be a challenge when conducting ambient measurements. As a result, O_2^- and SF_6^- were abandoned as potential reagent ions. Cl^-, I^-, and Br^- were also evaluated. It was expected that these reagent ions would form adducts with HO_2, of the form $X^-(HO_2)$. $Cl^-(HO_2)$ was not observed while utilizing Cl^- as a reagent ion, despite the detection of species commonly observed with negative reagent ions such as HNO_3 and CF_3COOH.

The I^- reagent ion, which has been used extensively to measure both organic and inorganic species (Huey et al., 1995;Slusher et al., 2004;Lee et al., 2014;Woodward-Massey et al., 2014;Brophy and Farmer, 2015;Faxon et al., 2015;Nah et al., 2016;Lee et

al., 2016), was found to cluster with HO_2, appearing at mass-to-charge 160, consistent with observations by Veres et al. (2015). However, it was observed that addition of NO_2 (Scott-Marrin, 100 ppm v/v N_2) to a clean N_2 gas matrix resulted in an increase of 1 cps per ppb NO_2 in the *m/z* 160 signal (normalized to a 10^6 cps I^- ion count rate). A 20 ppb addition results in a 20 cps increase in the *m/z* 160 signal, which is equivalent to ~4 ppt of HO_2. The addition of NO_2 showed an increase in a peak (*m/z* 159.9896) not associated with HO_2 that we could not identify. The addition of NO_2 did not affect the high resolution $I^-(HO_2)$ signal but is expected to be a significant artifact for instruments of low resolving power.

Unlike the other reagent ions, the Br^- ionization scheme was found to be sensitive to HO_2, the measurements were reproducible, and the signal did not respond to ppm level additions of NO_2 or O_3. The detection of HO_2 with Br^-, as well as its apparent robustness in the presence of common atmospheric constituents, made it an ideal candidate for further characterization.

3.2 Br^- ionization scheme characterization

3.2.1 Sensitivity

The instrument sensitivity to HO_2 using Br^- reagent was calibrated following the procedure in Sect. 2.2. Figure 3 shows HO_2 calibration curves for $^{79}Br^-(HO_2)$ at *m/z* 112.

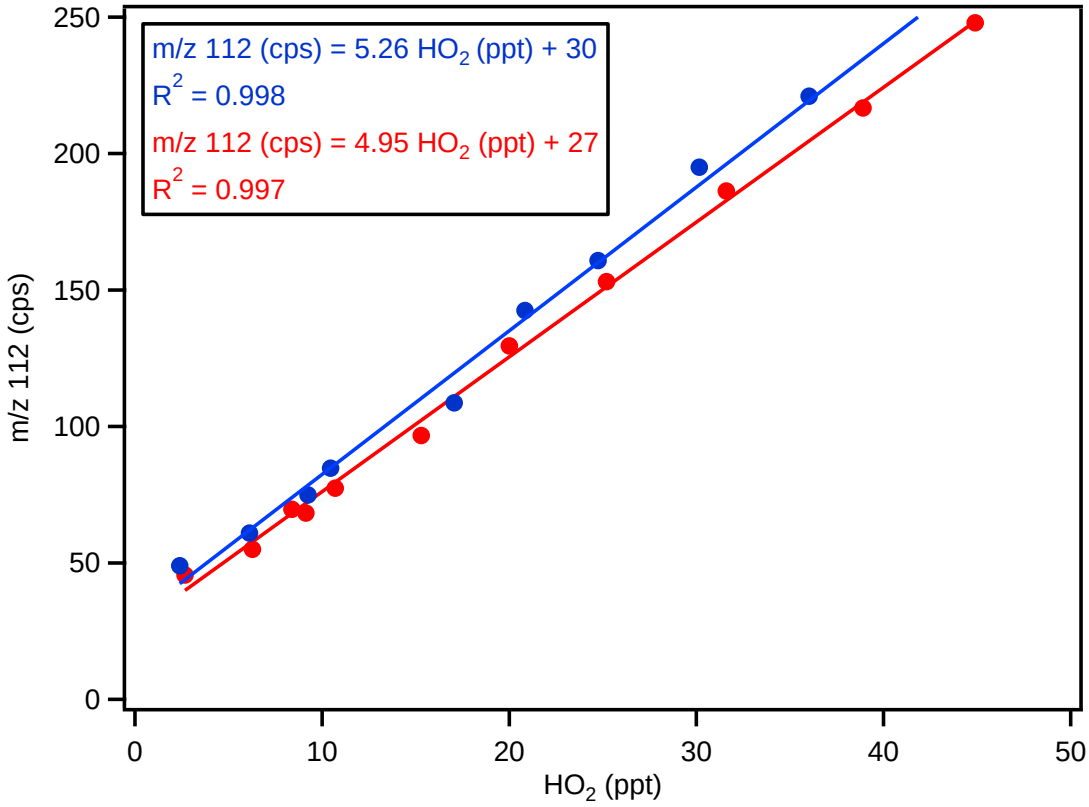

Figure 3: Laboratory HO_2 calibration curves for the $^{79}BrHO_2^-$ cluster as observed at nominal *m/z* 112. The slopes represent the sensitivity in cps/ppt. HO_2 mixing ratios are calculated using Eq. 1. The error associated with the individual sensitivities is 20% which arises from the combined uncertainty of the calibration parameters (Equation 1).

The curves are linear with slopes of 4.95±1.00 and 5.26±1.05 which represent the instrument sensitivity in cps/ppt for a $^{79}Br^-$ ion count of 10^6 cps. The two curves are shown to display the reproducibility of the calibration. Reproducible intercepts of 27±5 and 30±3 are observed for the calibration curves which are not explained by errors in any of the parameters used to calculate the expected HO_2 concentrations in Eq. 1. Instead, there appears to be a constant HO_2 photolytic source independent of water photolysis. The unidentified source requires the presence of water vapor but does not scale with the absolute water vapor mixing ratio. Furthermore, addition of 40 ppm C_3F_6 as an OH scavenger did not have an effect on the observed intercept, suggesting that the HO_2

production is unrelated to OH oxidation. The magnitude of the HO_2 formation from this unknown source scales linearly with the UV lamp flux. Most likely, the constant production of HO_2 leading to the intercept is from the photolysis of a carbonyl impurity in the gas. The intercept does not affect the sensitivity and is not used to calculate the HO_2 mixing ratio. Figure 4 is shown below to demonstrate the rapid instrument response to varying amounts of HO_2 during the calibrations.

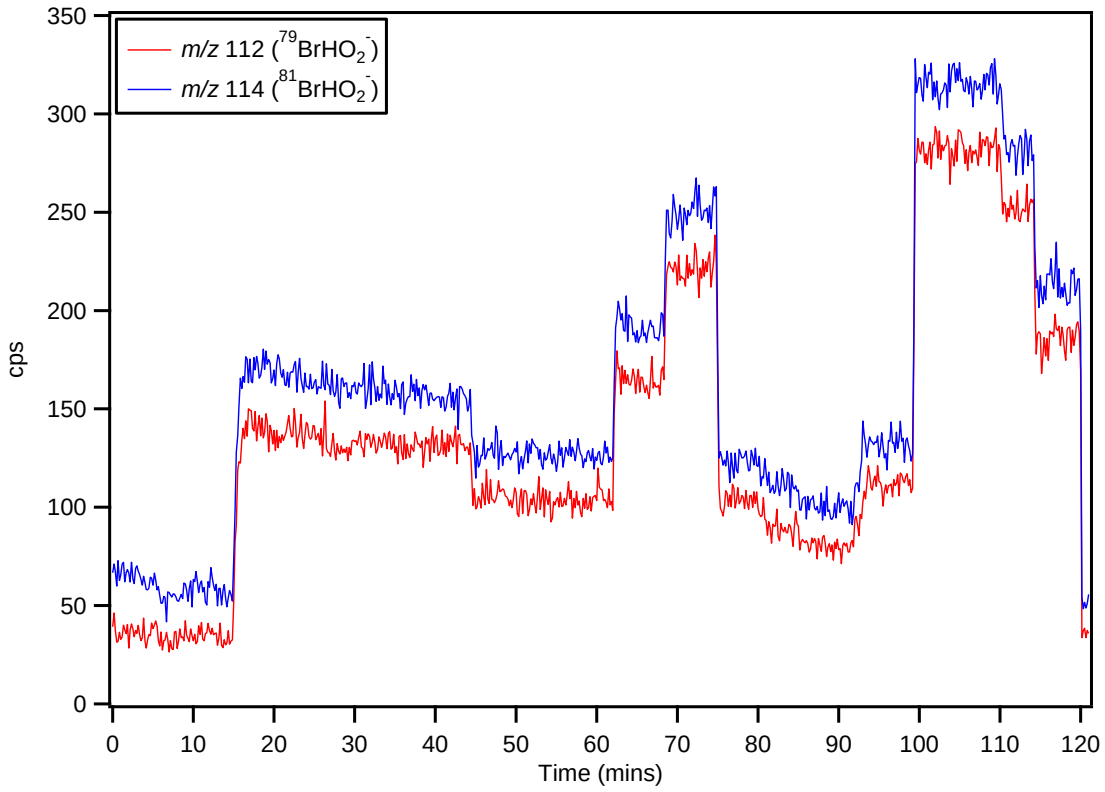

Figure 4: Time series of laboratory calibration of HO_2 at both mass-to-charges where HO_2 is observed. Points are averaged to 10 seconds to better display instrument response to changes in generated HO_2. At time zero, no HO_2 is being generated in the sample line. The mercury lamp is turned on at 15 minutes, resulting in an increase in signal. The small decrease in signal between 20 and 40 minutes is due to decreasing relative humidity in the sample line due to cooling in the bubbler from water evaporation. The lowest point above the background (~90 minutes) corresponds to 2.6 ppt of HO_2. The higher background associated with *m/z* 114 is due to contribution from the isotope of a trifluoroacetic acid (*m/z* 113) contamination associated with Teflon™ tubing.

3.2.2 Selectivity

The $Br^-(HO_2)$ measurement was found to be insensitive to NO_2 and O_3. A number of other common atmospheric constituents likely to behave as potential artifacts were also added to the sample flow to further explore the selectivity of the technique. Large concentrations (>10 ppm) of SO_2 were added, which did not elicit a response. Hydrogen peroxide and formaldehyde were sampled from the Georgia Tech Environmental Chamber facility (Boyd et al., 2015) at concentrations in excess of several ppm, eliciting responses of 0.25 cps/ppb and 0.002 cps/ppb, respectively. It is not clear whether the observed signal response is due to ion-molecule reaction with Br^- or unidentified wall reactions within the experimental chamber. Regardless, these responses are insignificant in the atmosphere and under most experimental conditions in the laboratory.

3.2.3 Effect of humidity and temperature on instrument sensitivity

Another important consideration for this technique is the effect of temperature and humidity on cluster stability, which was explored during laboratory characterizations. The effect of varying water vapor mixing ratios in the sample gas on sensitivity is shown in Figure 5.

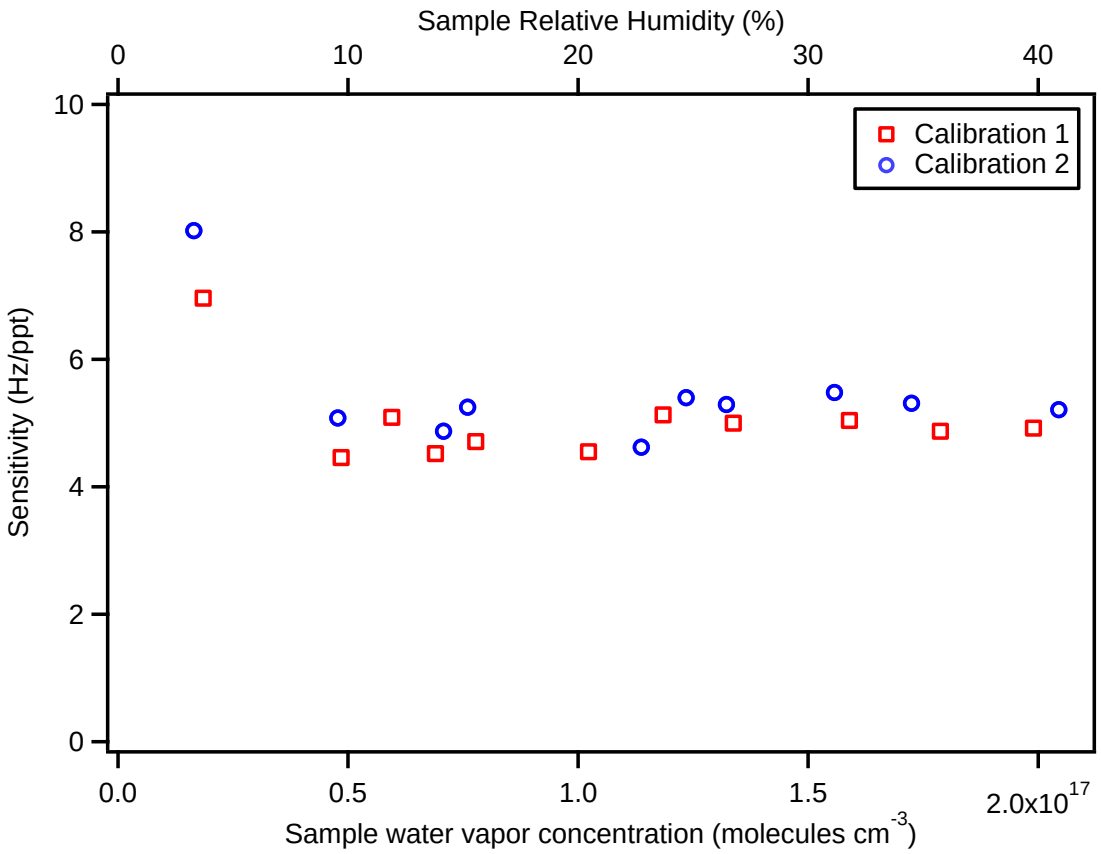

Figure 5: Instrument sensitivity as measured at *m/z* 112 $Br^-(HO_2)$ as a function of sample relative humidity. The instrument sensitivity demonstrates no water vapor dependence beyond a sample relative humidity of 10%. The "Calibration 1" and "Calibration 2" labels refer to the curves in Figure 3.

At sample relative humidities below 10%, the sensitivity appears to have a strong, negative water dependence. However, when the humidity in the sample gas is higher than 10%, the sensitivity is invariant with increasing relative humidity, which simplifies ambient sampling, as no humidity-dependent correction is required. The temperature dependence was also explored, where an IMR temperature increase from 20°C to 40°C resulted in a 20% decrease in instrument sensitivity. The relatively strong negative temperature dependence suggests that $Br^-(HO_2)$ is a weak cluster. This highlights the

importance of temperature control and performing calibrations at the sampling temperature.

3.3 Ambient measurements

3.3.1 Br^- ionization of ambient air

The diurnal profiles of HO_2, UV radiation index, NO, and O_3 for ambient sampling conducted in June 2015 in Atlanta are shown in Figure 6.

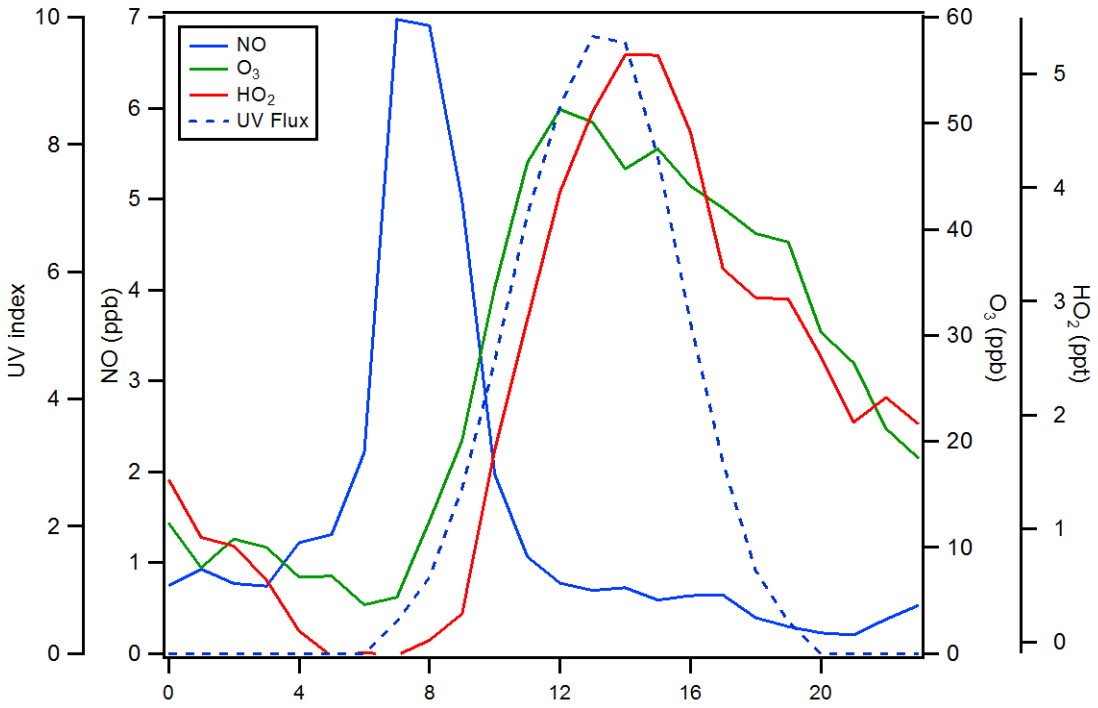

Figure 6: Hourly median diurnal profiles of HO_2, NO, O_3 and UV index in Atlanta. The sampling period was during 6/9/2015 21:14:00-6/11/2015 13:28:00, and 6/15/2015 1:52:00-6/25/2015 1:32:00 local time.

The HO_2 rises once the NO concentration is sufficiently low and peaks between 2 and 3 p.m. with a mixing ratio of ~5 ppt, comparable to previous studies in other urban regions (Emmerson et al., 2005;Kanaya et al., 2007;Dusanter et al., 2009). The 3σ limit

of detection was calculated to be 0.7 ppt for a 1 minute integration time based on laboratory calibrations (Section 3.2.1) and baselines observed during ambient sampling, which is sufficiently low for atmospherically important HO_2 concentrations. The slow decay of HO_2 in early evening may partially be explained by non-photolytic HO_2 production, e.g., from oxidation of biogenic volatile organic compounds (BVOCs), which are abundant in the Southeast United States (Geron et al., 2000;Guenther et al., 2006), as well as a decrease in boundary layer height. However, additional measurements would be required to constrain sources and sinks.

Mass spectra collected during ambient sampling and laboratory HO_2 calibrations in clean UHP N_2 gas are compared in Figure 7.

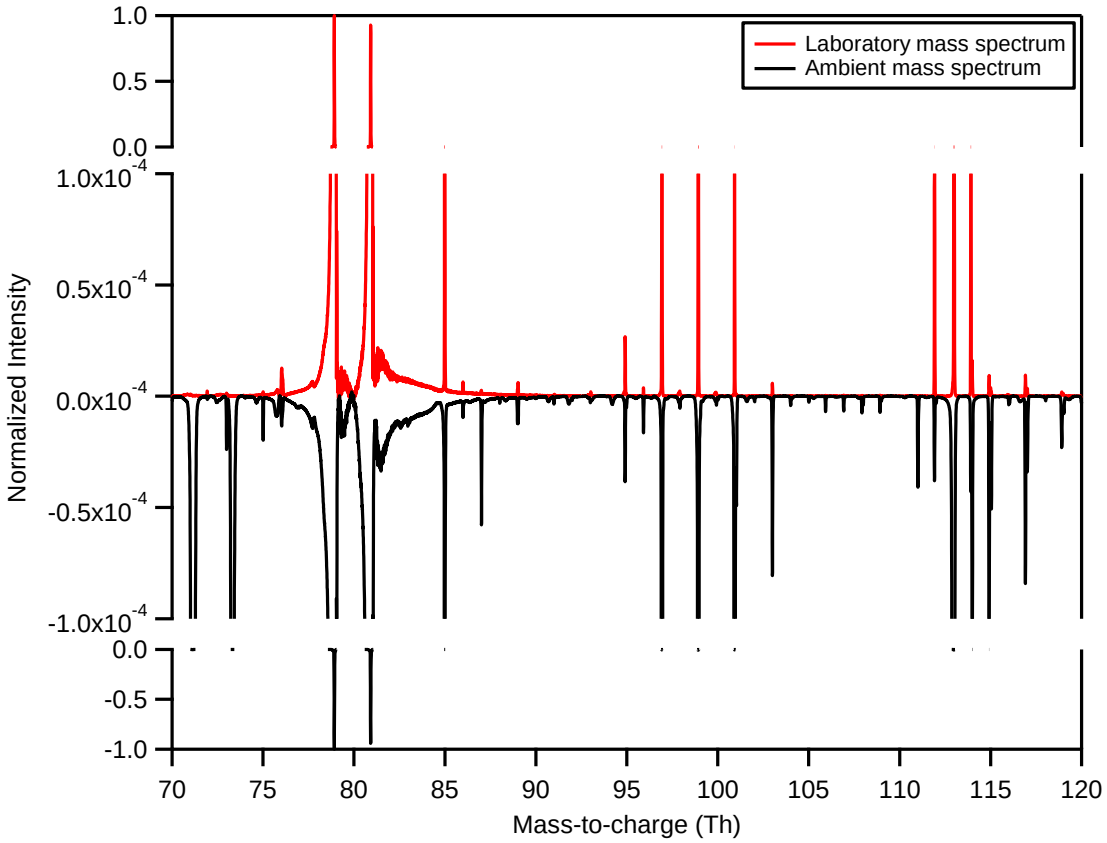

Figure 7: Comparison of laboratory generated and ambient mass spectra. Laboratory data was collected during HO_2 calibration using the procedure described in Sect. 3. Ambient data from a 24 hour period during ambient sampling is shown here. The ambient mass spectrum is reversed for clarity. Few additional peaks are observed in the ambient spectrum, the majority of which are of low signal intensity.

Few additional peaks are present in the ambient spectrum, suggesting that Br^- ionization is selective at the mass-to-charge values shown. Furthermore, the majority of additional peaks observed have signal intensities much lower than the intensity of the HO_2 signal at *m/z* 112, which makes it unlikely that the species at these additional peaks and their respective isotopes will affect the signal at *m/z* 112.

3.3.2 Inferring HO_2 and comparison to direct measurements

HNO_4 and NO_2 measurements were used to infer HO_2 concentrations for comparison with measured HO_2 concentrations. The HNO_4 and HO_2 are assumed to be in thermal equilibrium for the calculation. HO_2 concentration is calculated using Equation 2.

$$[HO_2] = \frac{[HNO_4]}{K(T)[NO_2]} \quad (2)$$

$K(T)$ represents the equilibrium constant and is a function of temperature alone (Burkholder et al. (2015). $K(T)$ in Eq. (S1) has a 30% uncertainty in this temperature range (Burkholder et al., 2015). The uncertainty of the HO_2NO_2 measurement was 16%, resulting in an overall uncertainty of 34% in the inferred HO_2 concentration. The precision of the NO_2 measurement is <100 ppt for a 10 s average time, thus the NO_2 measurement did not contribute significantly to the uncertainty of the inferred HO_2.

The validity of the equilibrium assumption made in Eq. S1 at the sampling site is determined by the time scale of fluctuations of NO and NO_2, which can be rapid given the site's proximity to an interstate.

During the period over which observations were made, the temperature was > 27°C and the lifetime of HNO_4 was less than 20 s. For the purpose of the comparison in Figure 8, the effects of deviations from equilibrium are expected to be small, given the use of hourly median values. The HO_2 diurnal profile calculated from Equation 2 is compared to the measured HO_2 diurnal profile in Figure 8.

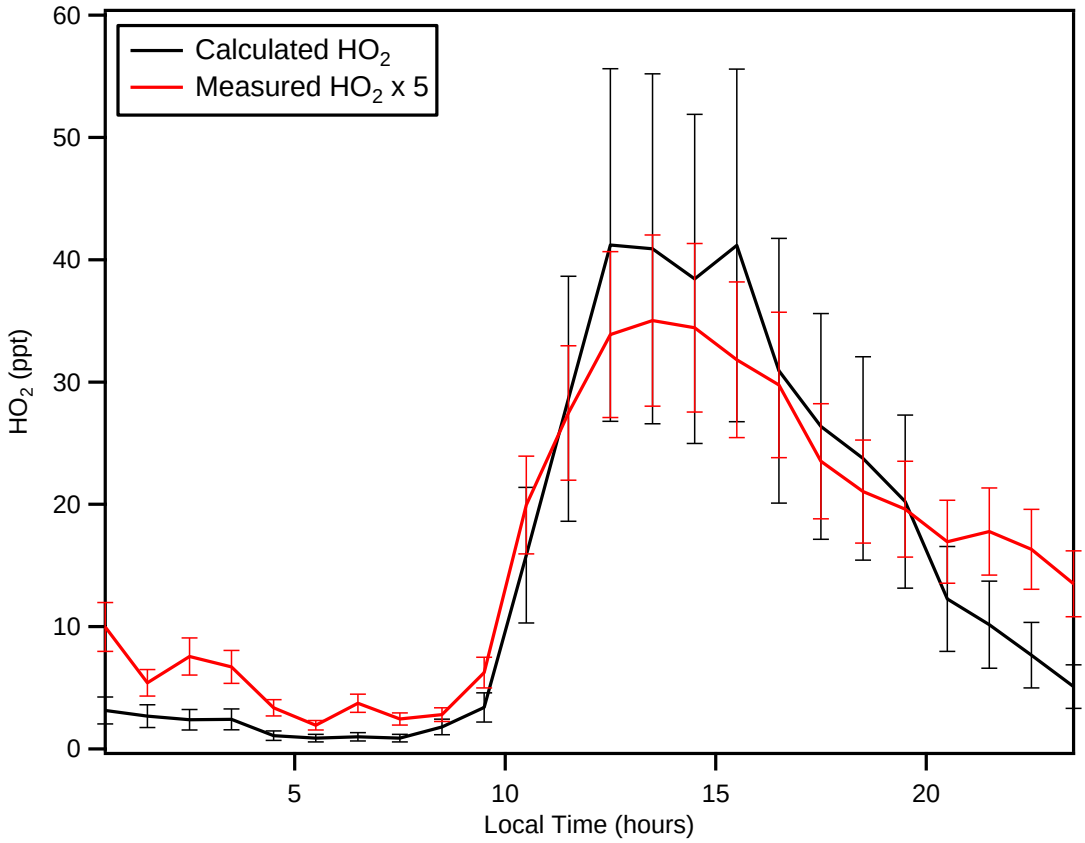

Figure 8: Comparison of HO_2 diurnal profiles (6/15/2015 to 6/18/2015) for measured HO_2 and HO_2 calculated assuming equilibrium between HO_2 and HNO_4. The measured HO_2 signal has been corrected by subtracting the contribution from internal generation of HO_2. The uncertainty in the measured HO_2 is attributed to the combined uncertainties from the calibration parameters in Eqn. 1. The uncertainty in calculated HO_2 only takes into account uncertainties in the equilibrium constant and the HNO_4 calibration.

The profiles agree well temporally, peaking during the same time of day, but not quantitatively, where they differ by a factor of 5 during the afternoon. The differences between the two profiles may be due to a number of factors. The sensitivity of the direct HO_2 measurement was determined in the laboratory and online calibrations were not conducted. It is possible that the sensitivity during ambient measurements was lower due to specific sampling conditions. In particular, the instrument experienced temperature changes between 20°C and 40°C, which decreased the sensitivity by 20%. Furthermore,

environmental conditions resulted in corrosion of the critical orifice on the HR-ToF-CIMS, which lowered the sample flow rate by 35%. The sensitivity was not corrected for the lower sample flow as the time at which the sample flow decreased was not known with certainty. The use of HNO_4 measurements to infer HO_2 has also not been validated. We have also observed some degree of interference in the HNO_4 measurement from NO_2, as well as a potentially larger interference from O_3 during laboratory characterizations. Nevertheless, the qualitative agreement between the two HO_2 profiles is encouraging and better constrained comparisons should be subject of future work.

3.3.3 Instrument background determinations

A final but important observation during our ambient measurements was that the measurement backgrounds differed between different background methods. We compared the measurement backgrounds obtained using two backgrounding methods: NO chemical titration by standard NO additions, and physical scrubbing using a metal wool scrubber. The NO titration of HO_2 resulted in lower background signals than physical scrubbing. Furthermore, additions of NO to the sample air after physical scrubbing further decreased the HO_2 signal. This suggests that there is internal HO_2 generation within the instrument. Laboratory characterizations were conducted to explore the discrepancy. In the laboratory, adding NO to a clean N_2 sample matrix also decreased the observed HO_2 background signal. The differences in HO_2 backgrounds observed between the different backgrounding methods and NO additions to N_2 gas were similar, representing ~4 ppt of HO_2 generated inside the instrument. The similarity suggests that HO_2 generation is independent of sample composition. The HO_2 is likely produced from ion-molecule reactions of trace gases in the N_2 used for ion generation. The

measurements of HO_2 presented in this work were post-corrected to account for internal generation.

3.4 Iodide-CIMS measurements of HO_2

Despite artifacts observed in the measurements of laboratory-generated HO_2, iodide ionization measurements were conducted during a short ambient sampling period to assess its viability in a real air matrix for the measurement of HO_2. The high resolution time series of the peak identified as $I^-(HO_2)$ is shown in Figure 9.

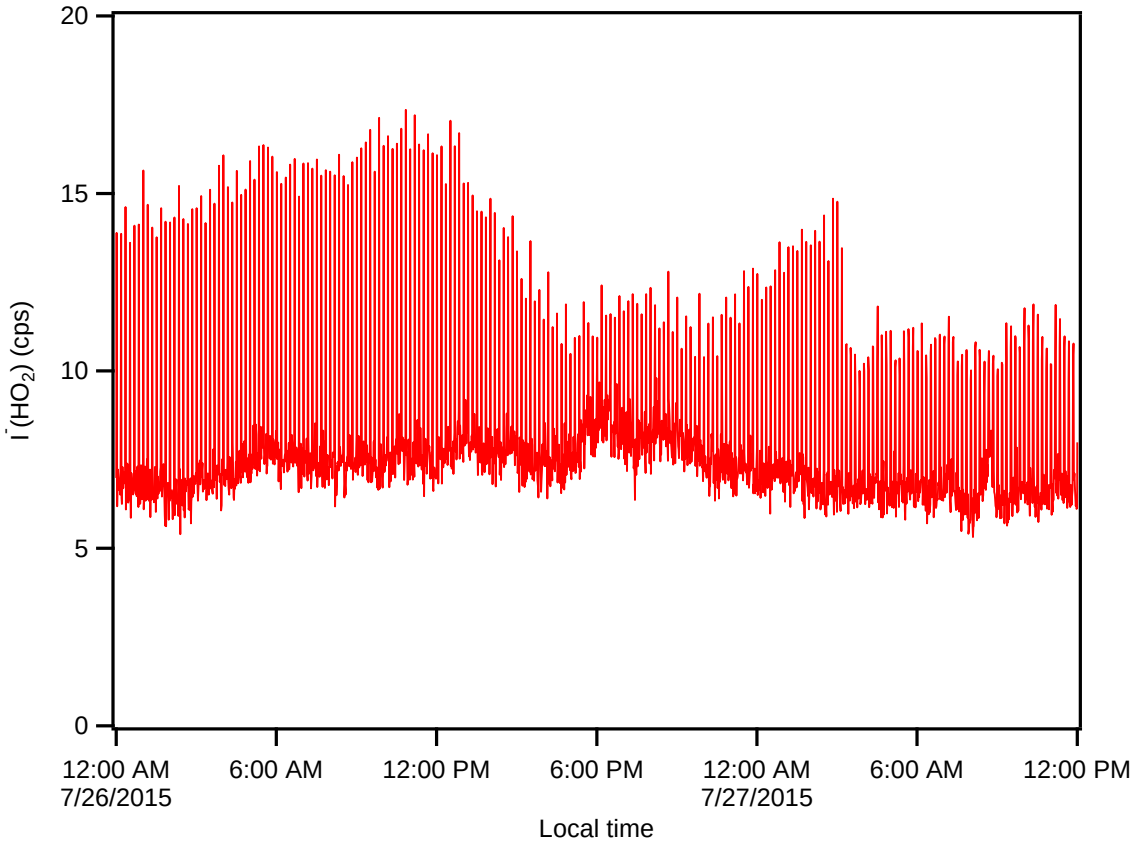

Figure 9: Time series of the high resolution $I^-(HO_2)$ peak intensity between 7/26/2015 12:00 a.m. to 7/27/2015 12:00 p.m. local time. The periodic increases in signal correspond to NO additions.

The behavior of the measured high resolution $I^-(HO_2)$ signal is not consistent with the expected behavior of HO_2. The time series do not show a clear diurnal pattern, nor is

the signal effectively suppressed by NO additions. Instead, NO additions caused the signal to increase. The high resolution capability of the HR-ToF-CIMS allowed for the peak assignment of $I^-(HO_2)$ with high accuracy, but the time-series of the high resolution peak displayed a similar behavior to that of the low resolution data. The resolving power of the instrument during the sampling period was ~3000 and the high resolution time series of the major peaks at nominal *m/z* 160 appear to be mostly independent of each other, which suggest that resolution is not a limiting factor. Additionally, a peak (*m/z* 159.990 Th) which may pertain to the NO_2-related artifact observed during earlier laboratory characterizations was present (Figure 10). Because the sampling period was short, the possibility of using iodide for HO_2 measurements may warrant further exploration. However, our laboratory and ambient measurements suggest that for iodide to be viable, high resolution capability will be necessary for accurate measurements due to artifacts caused by the presence of NO_2. This is not the case for Br^-. Figure 10 shows the mass spectra of Br^- and I^- at the mass-to-charge ratios where the HO_2 clusters are observed.

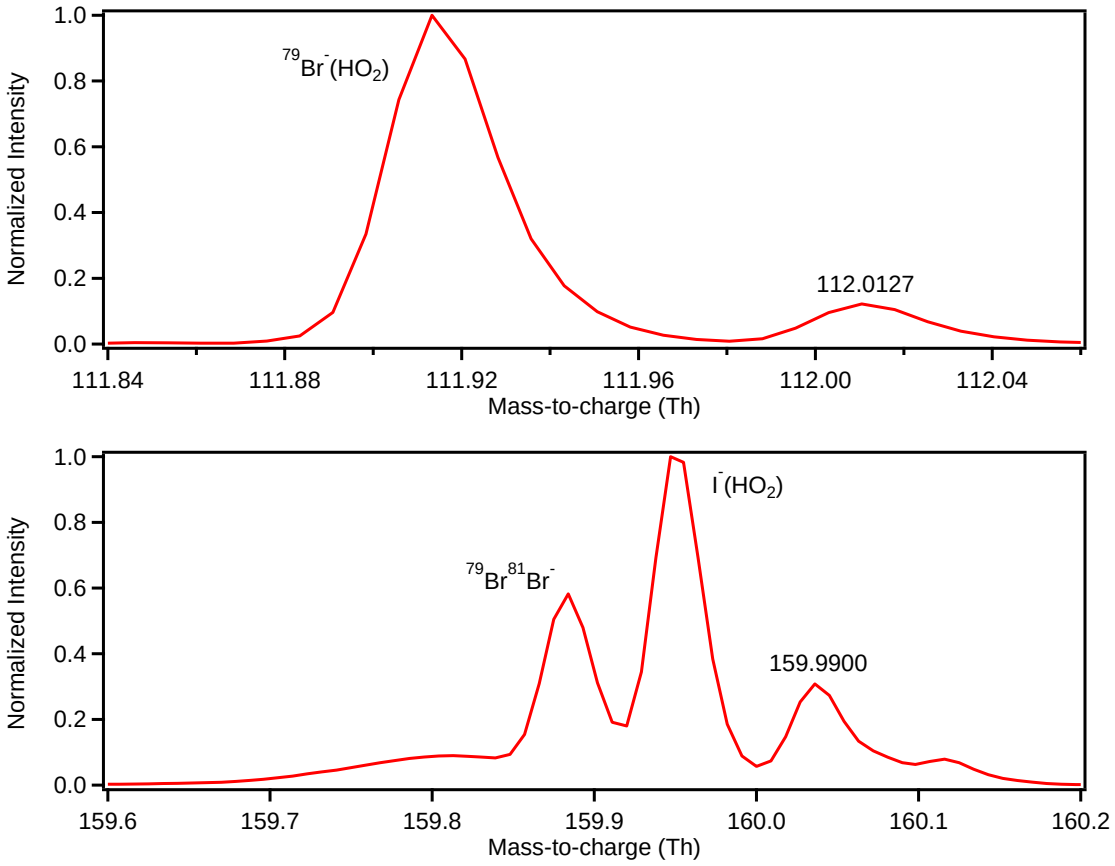

Figure 10: Normalized high resolution mass spectra of nominal *m/z* 112 for the Br^- ionization of HO_2 (top) and *m/z* 160 for the I^- ionization of HO_2 (bottom).

The Br^- spectrum shows that the $Br^-(HO_2)$ cluster is the dominant species at *m/z* 112. The minor peak observed is always present and does not vary significantly over the course of the day. Furthermore, the peak does not respond to NO additions, making NO backgrounds effective at eliminating any contribution to the signal from this peak. As a result, the measurement of HO_2 with Br^- does not require high resolution capability.

CHAPTER 4

CONCLUSIONS AND FUTURE DIRECTIONS

In this work, a number of negative reagent ions (O_2^-, SF_6^-, Cl^-, I^-, and Br^-) were evaluated for the detection of HO_2 using chemical ionization mass spectrometry. Reagent ions were evaluated on sensitivity and selectivity, as well as applicability to laboratory and ambient measurements of HO_2. Charge exchange was found to be a poor mechanism for the ionization of HO_2, as it did not produce a stable ion for transmission and detection. Clustering ionization proved to be a superior method for detecting HO_2. Among the reagent ions evaluated for cluster formation, Br^- was found to be the best candidate for the measurement of HO_2, providing improved selectivity over I^- in the presence of common atmospheric constituents.

Ambient measurements were conducted in Atlanta, GA in June 2015 to demonstrate the performance and capability of the instrument. The sensitivity using Br^- (5.1±1.00 cps/ppt per 10^6 ^{79}Br ion counts) was sufficient for ground-based measurements, resulting in a low 3σ detection limit of 0.7 ppt for 1 minute time resolution measurements. A comparison of ambient and laboratory generated mass spectra using Br^- demonstrated high selectivity over the range of mass-to-charge values important to HO_2 measurement. The HO_2 diurnal profile observed agreed with expectations, which suggests that no obvious artifacts are present in the HO_2 measurement. In addition, no other peaks of significant intensity were observed at *m/z* 112 in the high resolution mass spectra, demonstrating that high resolution instrumentation is not required for conducting HO_2 measurements using this technique.

Future work should revolve around the optimization of instrument sensitivity and characterization of the instrument background. A number of simple changes can be made to the CIMS instrument for improved sensitivity. Product ion transmission can be improved by increasing the sample flow through the nozzle leading to the SSQ chamber, a higher radioactivity source can be used, and an isotopically pure mixture of CF_3Br can be synthesized, among other possibilities.

Instrument background should be further characterized based on observations in this work, which showed internal HO_2 generation occurring in the radioactive source. Possible solutions to address internal HO_2 generation in determining the instrument background include utilizing a physical scrubber in place of chemical scrubbing or modulating the NO concentration in the sample line such that HO_2 in the sample is effectively removed while internally generated HO_2 is not allowed to react efficiently with NO. Pressures and sample flow rate to ion source flow rate ratios can be modified to suit this purpose. Alternatively, HO_2 generation may be suppressed by purification of the N_2 carrier gas or by the addition of a chosen reagent to the ion source flow. Future efforts should also aim to intercompare the Br-CIMS technique to other methods such as FAGE-LIF and MIESR in well-constrained atmospheric studies. The development of the Br-CIMS technique described here and future refinement represent a significant step in reconciling model-measurement discrepancies in HO_2, as well as facilitating the study of HO_2 chemistry in the laboratory.

APPENDIX A

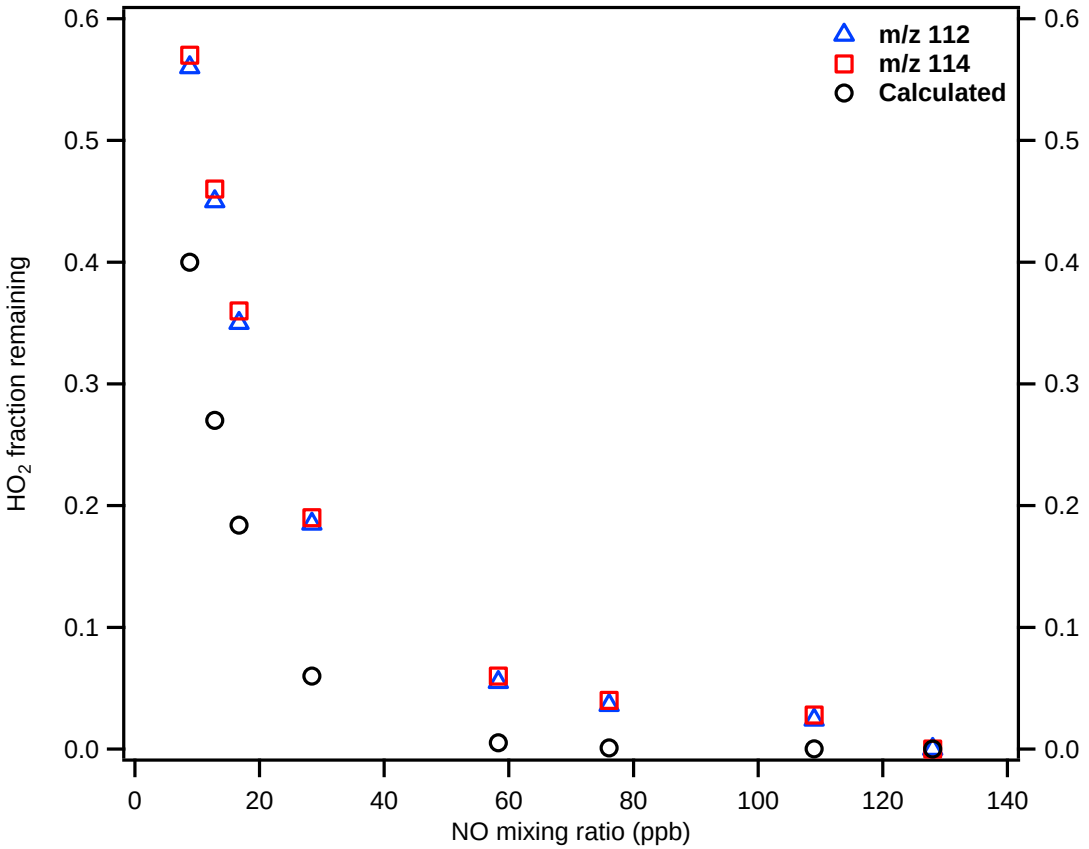

Figure 11: Effect of adding varying mixing ratios of NO on HO_2 signal. The y-axis shows the fraction of HO_2 signal remaining, observed at $^{79}Br^-(HO_2)$ (*m/z* 112) and $^{81}Br^-(HO_2)$ (*m/z* 114). The observed fraction remaining is compared to the calculated fraction remaining, assuming an effective reaction time equal to residence time of the flows before introduction into the instrument. The trend is consistent with expectation. The disagreement in absolute fraction remaining is explained by uncertainties in the effective reaction time due to mixing.

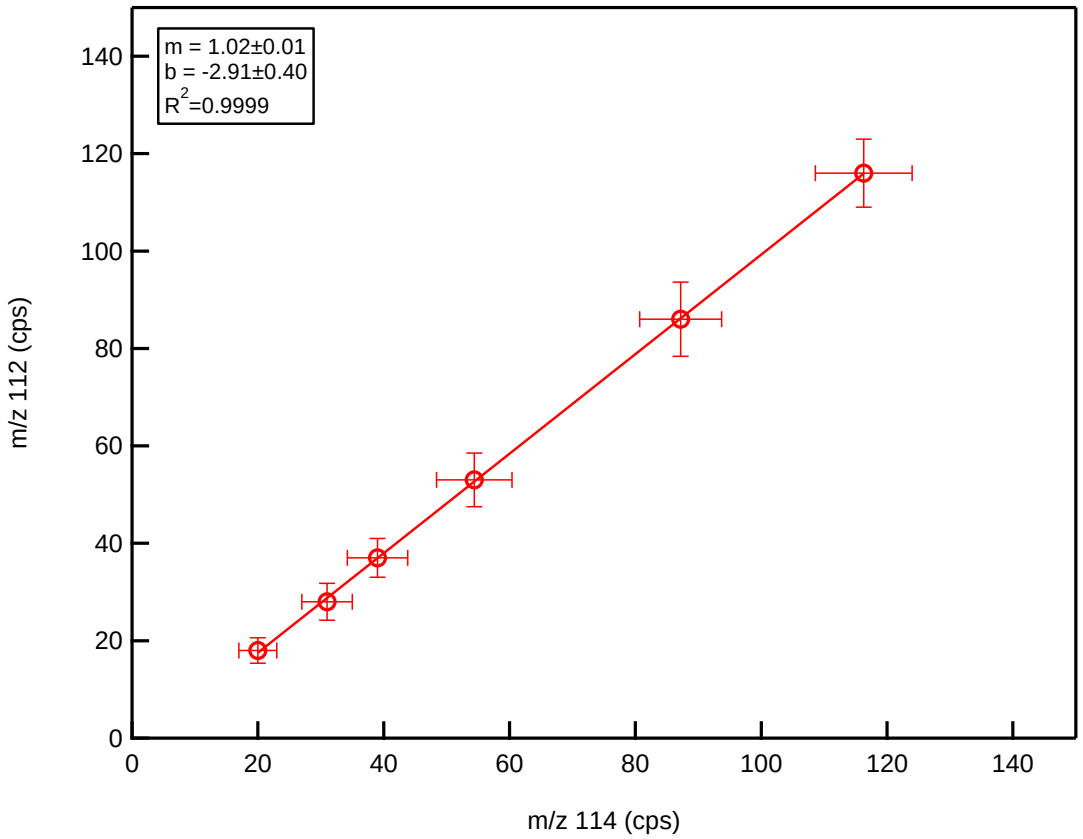

Figure 12: Comparison of $Br^{-}(HO_2)$ signal observed at m/z 112 and m/z 114. The linearity of the curve and the slope being equal to the isotopic abundance of ^{79}Br to ^{81}Br further confirm the identity of the cluster observed. The use of signals at both *m/z* 112 and *m/z* 114 is useful in confirming the absence of measurement artifacts in low resolution instruments.

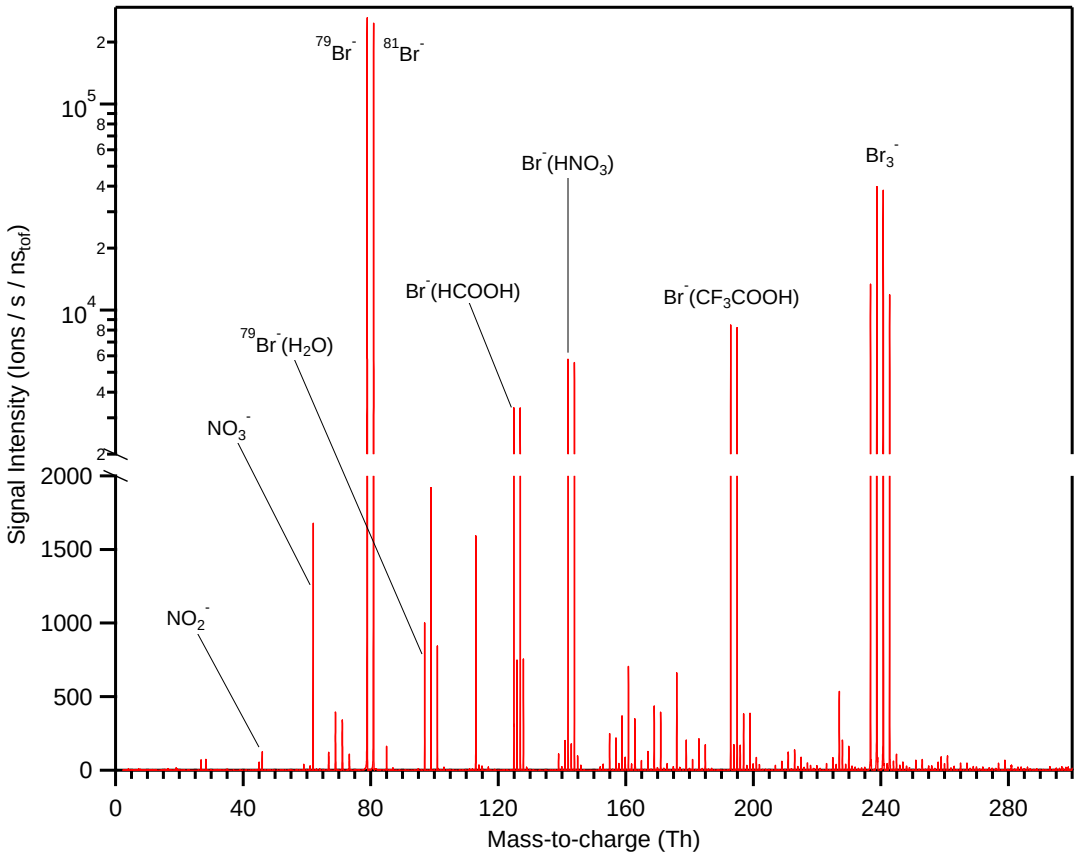

Figure 13: Full ambient mass spectrum for Br^- ionization up to *m/z* 300.

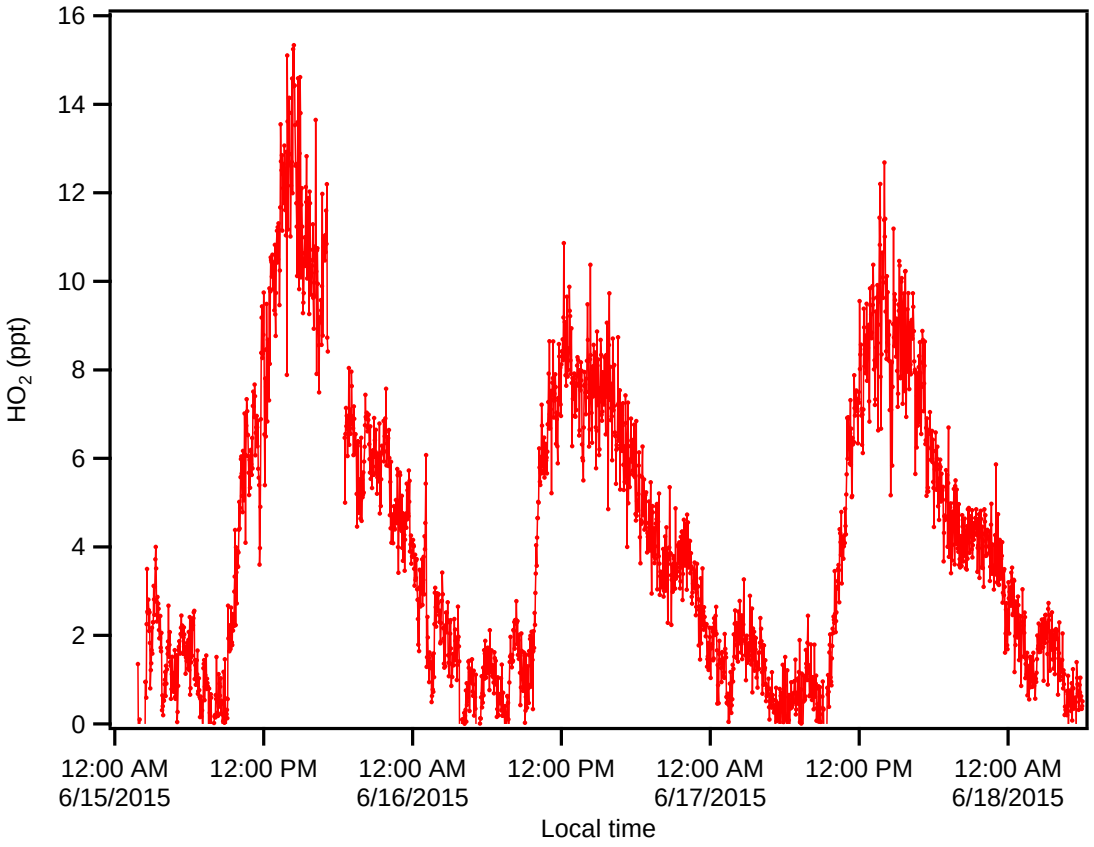

Figure 14: Time series of HO_2 for a 3 day sampling period.

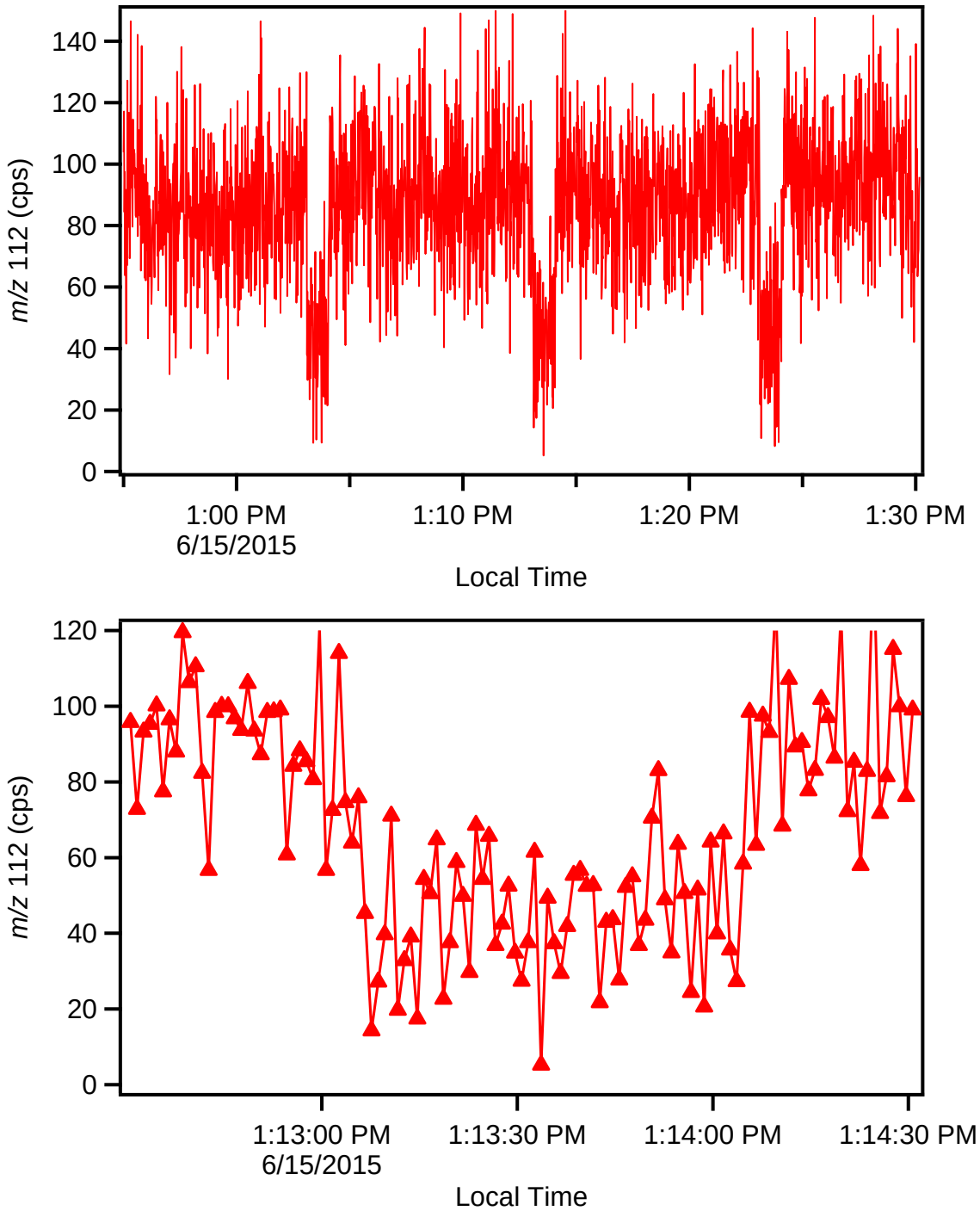

Figure 15: Example of instrument backgrounds obtained from the addition of NO. One second data are displayed. The top panel shows three consecutive background periods. The middle period is shown more closely in the bottom panel. Each marker represents a 1 second data point. The instrument response to NO additions is fast, ~2-4 seconds.

REFERENCES

Alam, M. S., Rickard, A. R., Camredon, M., Wyche, K. P., Carr, T., Hornsby, K. E., Monks, P. S., and Bloss, W. J.: Radical Product Yields from the Ozonolysis of Short Chain Alkenes under Atmospheric Boundary Layer Conditions, J Phys Chem A, 117, 12468-12483, 10.1021/jp408745h, 2013.

Arnold, S. T., and Viggiano, A. A.: Turbulent Ion Flow Tube Study of the Cluster-Mediated Reactions of SF6- with H2O, CH3OH, and C2H5OH from 50 to 500 Torr, The Journal of Physical Chemistry A, 105, 3527-3531, 10.1021/jp003967y, 2001.

Bertram, T. H., Kimmel, J. R., Crisp, T. A., Ryder, O. S., Yatavelli, R. L. N., Thornton, J. A., Cubison, M. J., Gonin, M., and Worsnop, D. R.: A field-deployable, chemical ionization time-of-flight mass spectrometer, Atmos. Meas. Tech., 4, 1471-1479, 10.5194/amt-4-1471-2011, 2011.

Boyd, C. M., Sanchez, J., Xu, L., Eugene, A. J., Nah, T., Tuet, W. Y., Guzman, M. I., and Ng, N. L.: Secondary organic aerosol formation from the β-pinene+NO3 system: effect of humidity and peroxy radical fate, Atmos. Chem. Phys., 15, 7497-7522, 10.5194/acp-15-7497-2015, 2015.

Brophy, P., and Farmer, D. K.: A switchable reagent ion high resolution time-of-flight chemical ionization mass spectrometer for real-time measurement of gas phase oxidized species: characterization from the 2013 southern oxidant and aerosol study, Atmos. Meas. Tech., 8, 2945-2959, 10.5194/amt-8-2945-2015, 2015.

Brune, W. H., Stevens, P. S., and Mather, J. H.: MEASURING OH AND HO2 IN THE TROPOSPHERE BY LASER-INDUCED FLUORESCENCE AT LOW-PRESSURE, Journal of the Atmospheric Sciences, 52, 3328-3336, 10.1175/1520-0469(1995)052<3328:moahit>2.0.co;2, 1995.

Burkholder, J. B., Sander, S. P., Abbatt, J., Barker, J. R., Huie, R. E., Kolb, C. E., Kurylo, M. J., Orkin, V. L., Wilmouth, D. M., and Wine, P. H.: "Chemical Kinetics and Photochemical Data for Use in Atmospheric Studies, Evaluation No. 18,"JPL Publication 15-10, Jet Propulsion Laboratory, Pasadena, 2015.

Cantrell, C. A., and Stedman, D. H.: A possible technique for the measurement of atmospheric peroxy radicals, Geophysical Research Letters, 9, 846-849, 10.1029/GL009i008p00846, 1982.

Cantrell, C. A., Stedman, D. H., and Wendel, G. J.: Measurement of Atmospheric Peroxy-Radicals by Chemical Amplification, Anal Chem, 56, 1496-1502, Doi 10.1021/Ac00272a065, 1984.

Cooke, M. C., Utembe, S. R., Carbajo, P. G., Archibald, A. T., Orr-Ewing, A. J., Jenkin, M. E., Derwent, R. G., Lary, D. J., and Shallcross, D. E.: Impacts of formaldehyde

photolysis rates on tropospheric chemistry, Atmospheric Science Letters, 11, 33-38, 10.1002/asl.251, 2010.

Creasey, D. J., Heard, D. E., and Lee, J. D.: Absorption cross-section measurements of water vapour and oxygen at 185 nm. Implications for the calibration of field instruments to measure OH, HO2 and RO2 radicals, Geophysical Research Letters, 27, 1651-1654, 10.1029/1999GL011014, 2000.

Crounse, J. D., Paulot, F., Kjaergaard, H. G., and Wennberg, P. O.: Peroxy radical isomerization in the oxidation of isoprene, Phys Chem Chem Phys, 13, 13607-13613, Doi 10.1039/C1cp21330j, 2011.

Docherty, K. S., Wu, W., Lim, Y. B., and Ziemann, P. J.: Contributions of Organic Peroxides to Secondary Aerosol Formed from Reactions of Monoterpenes with O3, Environ Sci Technol, 39, 4049-4059, 10.1021/es050228s, 2005.

Dusanter, S., Vimal, D., and Stevens, P. S.: Technical note: Measuring tropospheric OH and HO2 by laser-induced fluorescence at low pressure. A comparison of calibration techniques, Atmos. Chem. Phys., 8, 321-340, 10.5194/acp-8-321-2008, 2008.

Dusanter, S., Vimal, D., Stevens, P. S., Volkamer, R., and Molina, L. T.: Measurements of OH and HO2 concentrations during the MCMA-2006 field campaign – Part 1: Deployment of the Indiana University laser-induced fluorescence instrument, Atmos. Chem. Phys., 9, 1665-1685, 10.5194/acp-9-1665-2009, 2009.

Edwards, G. D., Cantrell, C. A., Stephens, S., Hill, B., Goyea, O., Shetter, R. E., Mauldin, R. L., Kosciuch, E., Tanner, D. J., and Eisele, F. L.: Chemical ionization mass spectrometer instrument for the measurement of tropospheric HO2 and RO2, Anal Chem, 75, 5317-5327, Doi 10.1021/Ac034402b, 2003.

Emmerson, K. M., Carslaw, N., Carpenter, L. J., Heard, D. E., Lee, J. D., and Pilling, M. J.: Urban Atmospheric Chemistry During the PUMA Campaign 1: Comparison of Modelled OH and HO2 Concentrations with Measurements, J Atmos Chem, 52, 143-164, 10.1007/s10874-005-1322-3, 2005.

Faxon, C. B., Bean, J. K., and Ruiz, L. H.: Inland Concentrations of Cl-2 and ClNO2 in Southeast Texas Suggest Chlorine Chemistry Significantly Contributes to Atmospheric Reactivity, Atmosphere-Basel, 6, 1487-1506, 10.3390/atmos6101487, 2015.

Fuchs, H., Bohn, B., Hofzumahaus, A., Holland, F., Lu, K. D., Nehr, S., Rohrer, F., and Wahner, A.: Detection of HO2 by laser-induced fluorescence: calibration and interferences from RO2 radicals, Atmos. Meas. Tech., 4, 1209-1225, 10.5194/amt-4-1209-2011, 2011.

Geron, C., Rasmussen, R., Arnts, R. R., and Guenther, A.: A review and synthesis of monoterpene speciation from forests in the United States, Atmospheric Environment, 34, 1761-1781, Doi 10.1016/S1352-2310(99)00364-7, 2000.

Geyer, A., Bachmann, K., Hofzumahaus, A., Holland, F., Konrad, S., Klupfel, T., Patz, H. W., Perner, D., Mihelcic, D., Schafer, H. J., Volz-Thomas, A., and Platt, U.: Nighttime formation of peroxy and hydroxyl radicals during the BERLIOZ campaign: Observations and modeling studies, J Geophys Res-Atmos, 108, 10.1029/2001jd000656, 2003.

Griffith, S. M., Hansen, R. F., Dusanter, S., Stevens, P. S., Alaghmand, M., Bertman, S. B., Carroll, M. A., Erickson, M., Galloway, M., Grossberg, N., Hottle, J., Hou, J., Jobson, B. T., Kammrath, A., Keutsch, F. N., Lefer, B. L., Mielke, L. H., O'Brien, A., Shepson, P. B., Thurlow, M., Wallace, W., Zhang, N., and Zhou, X. L.: OH and HO2 radical chemistry during PROPHET 2008 and CABINEX 2009 – Part 1: Measurements and model comparison, Atmos. Chem. Phys., 13, 5403-5423, 10.5194/acp-13-5403-2013, 2013.

Guenther, A., Karl, T., Harley, P., Wiedinmyer, C., Palmer, P. I., and Geron, C.: Estimates of global terrestrial isoprene emissions using MEGAN (Model of Emissions of Gases and Aerosols from Nature), Atmos Chem Phys, 6, 3181-3210, 2006.

Hanke, M., Uecker, J., Reiner, T., and Arnold, F.: Atmospheric peroxy radicals: ROXMAS, a new mass-spectrometric methodology for speciated measurements of HO2 and Sigma RO2 and first results, Int J Mass Spectrom, 213, 91-99, 10.1016/S1387-3806(01)00548-6, 2002.

Hennigan, C. J., Bergin, M. H., Dibb, J. E., and Weber, R. J.: Enhanced secondary organic aerosol formation due to water uptake by fine particles, Geophysical Research Letters, 35, n/a-n/a, 10.1029/2008GL035046, 2008.

Holland, F., Hofzumahaus, A., Schäfer, J., Kraus, A., and Pätz, H.-W.: Measurements of OH and HO2 radical concentrations and photolysis frequencies during BERLIOZ, Journal of Geophysical Research: Atmospheres, 108, PHO 2-1-PHO 2-23, 10.1029/2001JD001393, 2003.

Hornbrook, R. S., Crawford, J. H., Edwards, G. D., Goyea, O., Mauldin, R. L., Olson, J. S., and Cantrell, C. A.: Measurements of tropospheric HO2 and RO2 by oxygen dilution modulation and chemical ionization mass spectrometry, Atmos Meas Tech, 4, 735-756, DOI 10.5194/amt-4-735-2011, 2011.

Horstjann, M., Andrés Hernández, M. D., Nenakhov, V., Chrobry, A., and Burrows, J. P.: Peroxy radical detection for airborne atmospheric measurements using absorption spectroscopy of NO2, Atmos. Meas. Tech., 7, 1245-1257, 10.5194/amt-7-1245-2014, 2014.

Huey, L. G., Hanson, D. R., and Howard, C. J.: Reactions of SF6- and I- with Atmospheric Trace Gases, The Journal of Physical Chemistry, 99, 5001-5008, 10.1021/j100014a021, 1995.

J. Peeters, T. L. N. a. L. V.: HOx radical regeneration in the oxidation of isoprene, Phys Chem Chem Phys, 5935-5939, 2009.

Kanaya, Y., Cao, R., Akimoto, H., Fukuda, M., Komazaki, Y., Yokouchi, Y., Koike, M., Tanimoto, H., Takegawa, N., and Kondo, Y.: Urban photochemistry in central Tokyo: 1. Observed and modeled OH and HO2 radical concentrations during the winter and summer of 2004, Journal of Geophysical Research: Atmospheres, 112, n/a-n/a, 10.1029/2007JD008670, 2007.

Kim, S., Wolfe, G. M., Mauldin, L., Cantrell, C., Guenther, A., Karl, T., Turnipseed, A., Greenberg, J., Hall, S. R., Ullmann, K., Apel, E., Hornbrook, R., Kajii, Y., Nakashima, Y., Keutsch, F. N., DiGangi, J. P., Henry, S. B., Kaser, L., Schnitzhofer, R., Graus, M., Hansel, A., Zheng, W., and Flocke, F. F.: Evaluation of HO_x sources and cycling using measurement-constrained model calculations in a 2-methyl-3-butene-2-ol (MBO) and monoterpene (MT) dominated ecosystem, Atmos. Chem. Phys., 13, 2031-2044, 10.5194/acp-13-2031-2013, 2013.

Kroll, J. H., and Seinfeld, J. H.: Chemistry of secondary organic aerosol: Formation and evolution of low-volatility organics in the atmosphere, Atmospheric Environment, 42, 3593-3624, DOI 10.1016/j.atmosenv.2008.01.003, 2008.

Lee, B. H., Lopez-Hilfiker, F. D., Mohr, C., Kurten, T., Worsnop, D. R., and Thornton, J. A.: An Iodide-Adduct High-Resolution Time-of-Flight Chemical-Ionization Mass Spectrometer: Application to Atmospheric Inorganic and Organic Compounds, Environ Sci Technol, 48, 6309-6317, 10.1021/es500362a, 2014.

Lee, B. H., Mohr, C., Lopez-Hilfiker, F. D., Lutz, A., Hallquist, M., Lee, L., Romer, P., Cohen, R. C., Iyer, S., Kurtén, T., Hu, W., Day, D. A., Campuzano-Jost, P., Jimenez, J. L., Xu, L., Ng, N. L., Guo, H., Weber, R. J., Wild, R. J., Brown, S. S., Koss, A., de Gouw, J., Olson, K., Goldstein, A. H., Seco, R., Kim, S., McAvey, K., Shepson, P. B., Starn, T., Baumann, K., Edgerton, E. S., Liu, J., Shilling, J. E., Miller, D. O., Brune, W., Schobesberger, S., D'Ambro, E. L., and Thornton, J. A.: Highly functionalized organic nitrates in the southeast United States: Contribution to secondary organic aerosol and reactive nitrogen budgets, Proceedings of the National Academy of Sciences, 113, 1516-1521, 10.1073/pnas.1508108113, 2016.

Liu, Y., Morales-Cueto, R., Hargrove, J., Medina, D., and Zhang, J.: Measurements of Peroxy Radicals Using Chemical Amplification−Cavity Ringdown Spectroscopy, Environ Sci Technol, 43, 7791-7796, 10.1021/es901146t, 2009.

Matthews, P. S. J., Baeza-Romero, M. T., Whalley, L. K., and Heard, D. E.: Uptake of HO₂ radicals onto Arizona test dust particles using an aerosol flow tube, Atmos. Chem. Phys., 14, 7397-7408, 10.5194/acp-14-7397-2014, 2014.

Mihelcic, D., Ehhalt, D. H., Kulessa, G. F., Klomfass, J., Trainer, M., Schmidt, U., and Röhrs, H.: Measurements of free radicals in the atmosphere by matrix isolation and electron paramagnetic resonance, pure and applied geophysics, 116, 530-536, 10.1007/bf01636905, 1978.

Miyazaki, K., Parker, A. E., Fittschen, C., Monks, P. S., and Kajii, Y.: A new technique for the selective measurement of atmospheric peroxy radical concentrations of HO2 and RO2 using a denuding method, Atmos. Meas. Tech., 3, 1547-1554, 10.5194/amt-3-1547-2010, 2010.

Nah, T., Sanchez, J., Boyd, C. M., and Ng, N. L.: Photochemical Aging of α-pinene and β-pinene Secondary Organic Aerosol formed from Nitrate Radical Oxidation, Environ Sci Technol, 50, 222-231, 10.1021/acs.est.5b04594, 2016.

Orlando, J. J., and Tyndall, G. S.: Laboratory studies of organic peroxy radical chemistry: an overview with emphasis on recent issues of atmospheric significance, Chem Soc Rev, 41, 6294-6317, 10.1039/C2CS35166H, 2012.

Ramond, T. M., Blanksby, S. J., Kato, S., Bierbaum, V. M., Davico, G. E., Schwartz, R. L., Lineberger, W. C., and Ellison, G. B.: Heat of Formation of the Hydroperoxyl Radical HOO Via Negative Ion Studies†, The Journal of Physical Chemistry A, 106, 9641-9647, 10.1021/jp014614h, 2002.

Seeley, J. V., Meads, R. F., Elrod, M. J., and Molina, M. J.: Temperature and Pressure Dependence of the Rate Constant for the HO2 + NO Reaction, The Journal of Physical Chemistry, 100, 4026-4031, 10.1021/jp952553f, 1996.

Slusher, D. L., Pitteri, S. J., Haman, B. J., Tanner, D. J., and Huey, L. G.: A chemical ionization technique for measurement of pernitric acid in the upper troposphere and the polar boundary layer, Geophysical Research Letters, 28, 3875-3878, 10.1029/2001GL013443, 2001.

Slusher, D. L., Huey, L. G., Tanner, D. J., Flocke, F. M., and Roberts, J. M.: A thermal dissociation–chemical ionization mass spectrometry (TD-CIMS) technique for the simultaneous measurement of peroxyacyl nitrates and dinitrogen pentoxide, Journal of Geophysical Research: Atmospheres, 109, D19315, 10.1029/2004JD004670, 2004.

Smith, S. C., Lee, J. D., Bloss, W. J., Johnson, G. P., Ingham, T., and Heard, D. E.: Concentrations of OH and HO2 radicals during NAMBLEX: measurements and steady state analysis, Atmos. Chem. Phys., 6, 1435-1453, 10.5194/acp-6-1435-2006, 2006.

Stevens, P. S., Mather, J. H., and Brune, W. H.: Measurement of tropospheric OH and HO2 by laser-induced fluorescence at low pressure, Journal of Geophysical Research: Atmospheres, 99, 3543-3557, 10.1029/93JD03342, 1994.

Stone, D., Whalley, L. K., and Heard, D. E.: Tropospheric OH and HO2 radicals: field measurements and model comparisons, Chem Soc Rev, 41, 6348-6404, 10.1039/C2CS35140D, 2012.

Stone, D., Evans, M. J., Walker, H., Ingham, T., Vaughan, S., Ouyang, B., Kennedy, O. J., McLeod, M. W., Jones, R. L., Hopkins, J., Punjabi, S., Lidster, R., Hamilton, J. F., Lee, J. D., Lewis, A. C., Carpenter, L. J., Forster, G., Oram, D. E., Reeves, C. E., Bauguitte, S., Morgan, W., Coe, H., Aruffo, E., Dari-Salisburgo, C., Giammaria, F., Di Carlo, P., and Heard, D. E.: Radical chemistry at night: comparisons between observed and modelled HOx, NO3 and N2O5 during the RONOCO project, Atmos Chem Phys, 14, 1299-1321, 10.5194/acp-14-1299-2014, 2014.

Taketani, F., Kanaya, Y., and Akimoto, H.: Kinetic Studies of Heterogeneous Reaction of HO2 Radical by Dicarboxylic Acid Particles, Int J Chem Kinet, 45, 560-565, 10.1002/kin.20783, 2013.

Tanner, D. J., Jefferson, A., and Eisele, F. L.: Selected ion chemical ionization mass spectrometric measurement of OH, Journal of Geophysical Research: Atmospheres, 102, 6415-6425, 10.1029/96JD03919, 1997.

Veres, P. R., Roberts, J. M., Wild, R. J., Edwards, P. M., Brown, S. S., Bates, T. S., Quinn, P. K., Johnson, J. E., Zamora, R. J., and de Gouw, J.: Peroxynitric acid (HO2NO2) measurements during the UBWOS 2013 and 2014 studies using iodide ion chemical ionization mass spectrometry, Atmos. Chem. Phys., 15, 8101-8114, 10.5194/acp-15-8101-2015, 2015.

Volkamer, R., Sheehy, P., Molina, L. T., and Molina, M. J.: Oxidative capacity of the Mexico City atmosphere - Part 1: A radical source perspective, Atmos Chem Phys, 10, 6969-6991, 10.5194/acp-10-6969-2010, 2010.

Walker, H. M., Stone, D., Ingham, T., Vaughan, S., Cain, M., Jones, R. L., Kennedy, O. J., McLeod, M., Ouyang, B., Pyle, J., Bauguitte, S., Bandy, B., Forster, G., Evans, M. J., Hamilton, J. F., Hopkins, J. R., Lee, J. D., Lewis, A. C., Lidster, R. T., Punjabi, S., Morgan, W. T., and Heard, D. E.: Night-time measurements of HOx during the RONOCO project and analysis of the sources of HO2, Atmos Chem Phys, 15, 8179-8200, 10.5194/acp-15-8179-2015, 2015.

Whalley, L. K., Blitz, M. A., Desservettaz, M., Seakins, P. W., and Heard, D. E.: Reporting the sensitivity of laser-induced fluorescence instruments used for HO2 detection to an interference from RO2 radicals and introducing a novel approach that enables HO2 and certain RO2 types to be selectively measured, Atmos. Meas. Tech., 6, 3425-3440, 10.5194/amt-6-3425-2013, 2013.

Wolfe, G. M., Cantrell, C., Kim, S., Mauldin, R. L., III, Karl, T., Harley, P., Turnipseed, A., Zheng, W., Flocke, F., Apel, E. C., Hornbrook, R. S., Hall, S. R., Ullmann, K., Henry, S. B., DiGangi, J. P., Boyle, E. S., Kaser, L., Schnitzhofer, R., Hansel, A., Graus, M., Nakashima, Y., Kajii, Y., Guenther, A., and Keutsch, F. N.: Missing peroxy radical sources within a summertime ponderosa pine forest, Atmos Chem Phys, 14, 4715-4732, 10.5194/acp-14-4715-2014, 2014.

Woodward-Massey, R., Taha, Y. M., Moussa, S. G., and Osthoff, H. D.: Comparison of negative-ion proton-transfer with iodide ion chemical ionization mass spectrometry for quantification of isocyanic acid in ambient air, Atmospheric Environment, 98, 693-703, 10.1016/j.atmosenv.2014.09.014, 2014.

Xu, L., Guo, H., Boyd, C. M., Klein, M., Bougiatioti, A., Cerully, K. M., Hite, J. R., Isaacman-VanWertz, G., Kreisberg, N. M., Knote, C., Olson, K., Koss, A., Goldstein, A. H., Hering, S. V., de Gouw, J., Baumann, K., Lee, S.-H., Nenes, A., Weber, R. J., and Ng, N. L.: Effects of anthropogenic emissions on aerosol formation from isoprene and monoterpenes in the southeastern United States, Proceedings of the National Academy of Sciences, 112, 37-42, 10.1073/pnas.1417609112, 2015a.

Xu, L., Suresh, S., Guo, H., Weber, R. J., and Ng, N. L.: Aerosol characterization over the southeastern United States using high-resolution aerosol mass spectrometry: spatial and seasonal variation of aerosol composition and sources with a focus on organic nitrates, Atmos. Chem. Phys., 15, 7307-7336, 10.5194/acp-15-7307-2015, 2015b.

Ziemann, P. J., and Atkinson, R.: Kinetics, products, and mechanisms of secondary organic aerosol formation, Chem Soc Rev, 41, 6582-6605, 10.1039/C2CS35122F, 2012.